

Discovering Psychological Dynamics: The Gaussian Graphical Model in Cross-sectional and Time-series Data

Sacha Epskamp,¹ Lourens J. Waldorp,¹ René Møttus,² Denny Borsboom¹

1. University of Amsterdam: Department of Psychological Methods

2. University of Edinburgh: Department of Psychology

Abstract

We introduce the Gaussian graphical model (GGM; an undirected network of partial correlation coefficients) and detail its utility as an exploratory data analysis tool. The GGM can highlight potential causal relationships between observed variables—psychological dynamics—in addition to showing predictive mediation. We describe the utility in 3 kinds of psychological datasets: datasets in which consecutive cases are assumed independent (e.g., cross-sectional data), temporally ordered datasets (e.g., $n = 1$ time series), and a mixture of the 2 (e.g., $n > 1$ time series). In time-series analysis, the GGM can be used to model the residual structure of a vector-autoregression analysis (VAR), also termed *graphical VAR*. Two network models can then be obtained: a temporal network and a contemporaneous network. When analyzing data from multiple subjects, a GGM can also be formed on the variance-covariance structure of stationary means—the between-subjects network. We argue that both the contemporaneous and between-subjects networks add valuable information and can highlight potential causal pathways. We propose estimation methods to obtain these networks, which we implement in the R packages *graphicalVAR* and *mlVAR*. The methods are showcased in four empirical examples, and simulation studies on these methods are included in the supplementary materials.

Keywords: time-series analysis; multilevel modeling; multivariate analysis; exploratory-data analysis; network modeling

There has been a surge of network models being applied to psychological datasets in recent years. This is consistent with a general call to conceptualize observed psychological processes not merely as indicative of latent common causes but rather as emergent behavior of complex, dynamical systems in which psychological, biological, and sociological components directly interact with each other (Borsboom et al., 2011; Cramer et al., 2012, 2010; Schmittmann et al., 2013; van der Maas et al., 2006). Such relationships are typically not known, and probabilistic network models (Koller and Friedman, 2009) are used to explore potential causal relationships between observables (Epskamp et al., 2015; van Borkulo et al., 2015).

2014)—the dynamics of psychology. In this paper we aim to provide a methodological introduction to a powerful probabilistic network model applicable in exploratory data analysis, the Gaussian graphical model (GGM), and to propose how it can be used and interpreted in the analysis of time-series data. The GGM is an increasingly popular tool used to analyze cross-sectional data, but it is not often employed to analyze time-series data. We show that in time-series modeling the GGM allows researchers to extend the modeling framework to incorporate contemporaneous and between-subjects effects. We do this by building up the model complexity in three steps: (1) when cases can be assumed to be independent (e.g., cross-sectional data or repeated measures in which no auto-regression is assumed), (2) temporally ordered data (e.g., $N = 1$ time-series data or $N > 1$ time-series data where no individual differences are assumed), and (3) temporally ordered data from multiple subjects (e.g., $N > 1$ time series). In each step, we describe estimation procedures and software packages that allow researchers to estimate these models. The use of GGM models in Step 3 is new, and we propose a novel estimation procedure to estimate these models, which we have implemented in two free software packages: *mlVAR*,¹ and *graphicalVAR*.²

We can currently distinguish two distinct and mostly separate lines of research in which networks are utilized on psychological datasets: the modeling of cross-sectional data and the modeling of intensive repeated measures in relatively short time frames (e.g., several times per day during several weeks). In cross-sectional modeling, a model is applied to a dataset in which multiple subjects are measured only once. The most popular method estimates undirected network models, indicating pairwise interactions—so-called pairwise Markov random fields (Epskamp et al., 2012; Murphy, 2012). When the data are continuous and assumed normally distributed, the GGM can be estimated. The GGM estimates a network of *partial correlation coefficients*—the correlation between two variables after conditioning on all other variables in the dataset (Epskamp et al., 2016a). This model is applied extensively to psychological data (e.g., Cramer et al. 2012; Fried et al. 2016; Isvoranu et al. 2016b; Kossakowski et al. 2015; McNally et al. 2015; van Borkulo et al. 2015). The GGM is an undirected network model and should be compared to directed network model estimation (e.g., Kalisch et al. 2012), in which estimating the direction of the effect is often cumbersome without reliance on stringent assumptions.

Researchers can obtain time-series data by using the experience sampling method (ESM; Myin-Germeys et al. 2009), in which subjects are asked several times per day to fill out a short questionnaire using a device or smartphone app. Often in ESM data, repeated measures of one or multiple participants are modeled through the use of (multilevel) vector autoregressive (VAR) models, which estimate how well each variable predicts the measured variables at the next time point (Borsboom and Cramer, 2013). These models are increasingly popular in assessing intraindividual dynamical structures (e.g., Bringmann et al. 2013, 2015; Wigman et al. 2015). A common misconception is that the GGM can only be applied to cross-sectional data. The GGM simply does not take temporal information into account, and its estimation relies on an assumption of the independence of cases. As we show below, the VAR model can be seen as a generalization of the GGM that takes violations of

¹CRAN link: <http://cran.r-project.org/package=mlVAR>

Github link (developmental): <http://www.github.com/SachaEpskamp/mlVAR>

²CRAN link: <http://cran.r-project.org/package=graphicalVAR>

Github link (developmental): <http://www.github.com/SachaEpskamp/graphicalVAR>

independence between consecutive cases into account. Thus, the lines of research on cross sectional and time-series data can be easily combined. The GGM offers a powerful tool to gain insight into potential dynamics at the contemporaneous time level via the use of an undirected network. Modeling the contemporaneous relationships from a VAR model using a GGM is called graphical VAR (Wild et al., 2010). Again, using a GGM in time-series data should be compared to using directed network structures at the contemporaneous time level (e.g., structural VAR; Chen et al. 2011b). We show that even when the data-generating process is a structural VAR model, using graphical VAR in exploratory data analysis offers more reliable insight into the potential contemporaneous dynamics.

When cases can be assumed to be independent, a single GGM network can readily be estimated from cross sectional or intraindividual data. Researchers can generalize this framework via the graphical VAR model for temporally ordered data in the case where two network structures can be obtained: the *temporal network*, a directed network indicating within-person relationships across time, and the *contemporaneous network*, an undirected GGM within the same measurement. When this framework is extended to multiple subject designs, a third network structure can be obtained: the *between-subjects network*, which is an undirected GGM between the means of the subject’s scores within the time span of measurement. Thus, analyzing the time-series of multiple subjects allows researchers to separate between-subjects effects as well as within-subjects temporal and within-subjects contemporaneous effects. We describe the utility of the contemporaneous and between-subjects network and how all three networks can highlight potential causal pathways, thereby acting as hypothesis-generating structures. We showcase the described methodology and software packages in four empirical examples by reanalyzing existing datasets (Bringmann et al., 2013; Geschwind et al., 2011; Kossakowski et al., 2017; Möttus et al., 2016; Revelle, 2010; Wichers et al., 2016). Finally, we assess the performance of these methods in large-scale simulation studies.

Notation

Throughout this paper we will employ the following notation. Roman letters indicate observed variables, and Greek letters indicate parameters or latent variables. Nonboldface letters indicate a single value. An uppercase nonboldface letter indicates a random variable, and a lowercase nonboldface letter indicates a realization. We use t ($t \in \{1, 2, \dots, n_t\}$) to denote measurement occasion and T to denote a random measurement occasion,³ i ($i \in \{1, 2, \dots, n_i\}$) to denote item administered and I to denote a random item, and p ($p \in \{1, 2, \dots, n_p\}$) to denote a subject and P to denote a random subject. Because n often denotes the number of subjects, we occasionally refer to n_p simply as n (e.g., $n = 1$ data). We will use lowercase boldface letters to denote column vectors and uppercase boldface vectors to denote matrices. Subscripts will denote if these are random or fixed. For example, \mathbf{B}_p will denote a fixed matrix for subject p , and \mathbf{B}_P will denote the matrix of random subject P (which has a distribution).

³Mostly we assume measurements are nested in subjects, and two subjects might have a different number of measurement occasions. As such, $t = 1$ for subject $p = 1$ might not correspond to $t = 1$ for subject $p = 2$. Adding sub- or superscripts to t and n_t might make this clear, but we have elected not to do so for notational clarity.

Because we are interested in finding dynamics between items, we use vector \mathbf{y} to denote the set of all items.⁴ For the observed variables, we will use consistent subscripts (measurement, subject) to denote which items are contained in the vector. For example, $\mathbf{y}_{[t,p]}$ denotes all responses of subject p at time point t , and $\mathbf{y}_{[T,p]}$ denotes all responses of subject p at a random time point T . A set in this subscript indicates multiple responses. For example, we will use $\mathbf{y}_{[\{t-1,t\},p]}^\top = [\mathbf{y}_{[t-1,p]}^\top \quad \mathbf{y}_{[t,p]}^\top]$ to denote a set of lagged and current responses from subject p around time point t . If only one observation or subject is measured, we will drop the square brackets (e.g., $\mathbf{y}_P = \mathbf{y}_{[1,P]}$ indicates the cross-sectional response pattern of a random subject). When it is unclear if the set of items corresponds to a random person or a random measurement occasion, we refer to C as a random case, with c as a particular case, and subset the data either as \mathbf{y}_C to describe a random response pattern or \mathbf{y}_c to describe a realization—in cross-sectional data $\mathbf{y}_C = \mathbf{y}_P$ and in $N = 1$ time-series data $\mathbf{y}_C = \mathbf{y}_T$. C could also indicate a set of multiple responses. Other subscripts denote subsets of a vector or matrix, with notation $-(\dots)$ indicating the subset of everything except $\{\dots\}$.

The Gaussian Graphical Model

Let $\mathbf{y}_C^\top = [Y_{C1} \ Y_{C1} \ \dots]$ denote a random vector with \mathbf{y}_c as its realization. We assume \mathbf{y}_C is centered and normally distributed with some variance–covariance matrix Σ :

$$\mathbf{y}_C \sim N(\mathbf{0}, \Sigma). \quad (1)$$

We currently do not define the nature of the observed variables. Thus, \mathbf{y}_C can consist of variables relating to one or more subjects, could contain repeated measures on one or more variables, could contain variables of a single subject that do not vary within-person, and so forth. Consider three examples: (1) Y_1 could represent the level of anxiety of subject p on Day 1 and Y_2 the level of anxiety of subject p on Day 2, (2) Y_1 could represent the length of subject p and Y_2 the number of times subject p bumps his or her head, and (3) Y_1 could represent the number of cigarettes subject p smokes per day and Y_2 the number of cigarettes another subject $p + 1$ smokes per day (case C then represents a dyadic pair).

Assuming multivariate normality, Σ encodes all the information necessary to determine how the observed measures relate to one another. However, we will not focus on Σ in this paper but rather on its inverse—the *precision matrix* \mathbf{K} ,

$$\mathbf{K} = \Sigma^{-1}.$$

Of particular importance is that the standardized elements of the precision matrix encode partial correlation coefficients of two variables, given all other variables (dropping subscript C for notational clarity):

$$\text{Cor}(Y_i, Y_j \mid \mathbf{y}_{-(i,j)}) = -\frac{\kappa_{ij}}{\sqrt{\kappa_{ii}}\sqrt{\kappa_{jj}}},$$

in which κ_{ij} denotes an element of \mathbf{K} , and $\mathbf{y}_{-(i,j)}$ denotes the set of variables without i and j . These partial correlations can be graphically displayed in a weighted network, in which

⁴If researchers are interested in dyadic interactions (Ferrer, 2016), for example, then a dyadic pair can be seen as a “subject,” and items can be the item responses from both subjects.

each variable Y_i is represented as a node, and connections (edges) between these nodes represent the partial correlation between two variables. When the partial correlation (thus the corresponding element in \mathbf{K}) equals zero, no edge is drawn. Thus, modeling the inverse variance–covariance matrix, such that every nonzero element is treated as a freely estimated parameter, allows for a sparse model for $\mathbf{\Sigma}$ (i.e., every element in $\mathbf{\Sigma}$ may be nonzero and some elements in \mathbf{K} are zero; Epskamp et al. 2016c). Such a model is termed a GGM (Lauritzen 1996).

When drawing a GGM as a network, positive partial correlations are typically visualized with blue or green edges and negative partial correlations with red edges,⁵ and the absolute strength of a partial correlation is represented by the width and saturation of an edge (Epskamp et al., 2012). When a partial correlation is zero, we draw no edge between two nodes. As such, the GGM can be seen as a network model of conditional associations; no edge indicates that two variables are independent after conditioning on all other variables in the dataset. This allows us to model conditional associations, which we might expect to be zero, rather than marginal associations, which we do not typically expect to be zero (especially in psychology).

To exemplify the above, suppose for three variables the true variance–covariance matrix is

$$\mathbf{\Sigma} = \begin{bmatrix} 1 & -0.26 & 0.31 \\ -0.26 & 1 & 0.08 \\ 0.31 & 0.08 & 1 \end{bmatrix}.$$

To estimate this matrix, we need three parameters (three covariances). The corresponding true precision matrix becomes

$$\mathbf{K} = \mathbf{\Sigma}^{-1} = \begin{bmatrix} 1.18 & 0.28 & -0.34 \\ 0.28 & 1.07 & 0 \\ -0.34 & 0 & 1.11 \end{bmatrix}.$$

Modeling \mathbf{K} would only require two parameters because one of the elements is zero. We can now standardize this matrix and make the off-diagonal elements negative to obtain the partial correlation matrix, which we will denote \mathbf{R} :

$$\mathbf{R} = \begin{bmatrix} 1 & -0.25 & 0.3 \\ -0.25 & 1 & 0 \\ 0.3 & 0 & 1 \end{bmatrix}.$$

This matrix can be used to draw a network as is shown in Figure 1. This figure shows that someone who is tired is also more likely to suffer from concentration problems and insomnia. Furthermore, this network shows that concentration problems and insomnia are conditionally independent given the level of fatigue.

⁵Many publications make use of the default color setup used in *qgraph* (Epskamp et al., 2012): green for positive edges and red for negative edges. A later version of *qgraph* includes the option `theme = "colorblind,"` using a more colorblind-friendly coloring scheme and setting the positive edge color to blue. This option has been used for all graphs in this paper. It should be noted that some publications also use blue and red edges but use red to denote positive and blue to denote negative effects akin to a heat map.

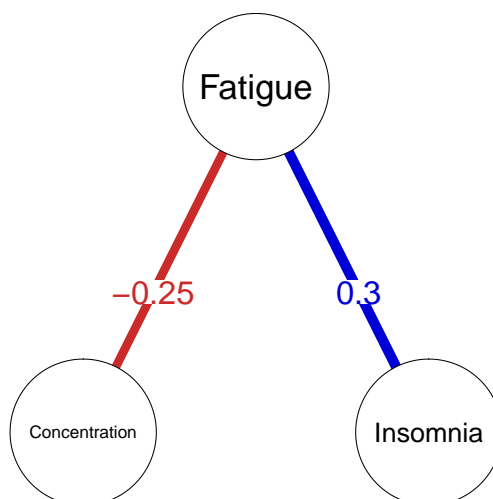


Figure 1. A hypothetical example of a GGM on psychological variables. Nodes represent someone’s ability to concentrate, someone’s level of fatigue, and someone’s level of insomnia. Connections between the nodes, termed *edges*, represent partial correlation coefficients between two variables after conditioning on the third. Blue edges indicate positive partial correlations, red edges indicate negative partial correlations, and the width and saturation of an edge corresponds to the absolute value of the partial correlation.

Because many elements in the GGM can be zero (conditional independence) while allowing for all elements of Σ to be nonzero, the GGM offers a powerful way of modeling Σ in a sparse manner without having to rely on a strong causal theory on the direction of the effects (Epskamp et al., 2016c). The use of undirected network models, rather than directed network models, in cases where the direction of causal effects is poorly identified helps us to discover psychological dynamics in several ways:

1. Causal effects between two variables lead to an edge in the GGM, and the absence of a causal effect between two variables often (but not always) leads to no edge in the GGM. Therefore, an edge in the GGM can be seen as indicative of potential causal pathways (we stress that the focus of this paper is exploratory hypothesis-generating research).
2. The GGM, unlike directed *causal models*, is well identified and does not feature equivalent models. Therefore, exploratory search algorithms are better at identifying a GGM model. As we will show, the direction of causal effect is often hard to estimate. The GGM does not have this problem because it imposes no direction on the effect.
3. When an edge is spurious, for example, due to the presence of an unobserved cause, the undirected network does not feature a troublesome directional interpretation. Instead,

the presence of common-cause structures in a dataset is represented by clusters (a set of nodes that are all connected to one another) in the GGM.

4. The GGM does not rely on a causal interpretation. The partial correlation coefficients can be regarded as proportional to multiple regression coefficients, predicting one node from all other nodes. As such, the GGM can always be interpreted to show predictive effects and offers a powerful exploratory tool to gain insight into potential mediation paths and to map out multicollinearity.
5. Undirected network models also allow for a causal interpretation, one of genuine symmetric effects, and have been used thusly in diverse scientific fields such as statistical physics.

We outline these five points in more detail below. First, we discuss Points 1 to 3 by exploring the relationship between the GGM and causal generating mechanisms. Next, we discuss Point 4 by showing how partial correlation coefficients correspond to multiple regression coefficients. Finally, we discuss Point 5 by describing a closely related model to the GGM: the Ising model.

The Gaussian Graphical Model and Causal Generating Structures

Let $\boldsymbol{\eta}_C$ represent a set of unobserved variables, which we assume to be jointly normally distributed with \mathbf{y}_C . Then, we can form an encompassing framework for several possible causal generating models:

$$\begin{aligned}\mathbf{y}_c &= \mathbf{B}\mathbf{y}_c + \mathbf{A}\boldsymbol{\eta}_c + \boldsymbol{\varepsilon}_c \\ \boldsymbol{\varepsilon}_C &\sim N(\mathbf{0}, \boldsymbol{\Theta}),\end{aligned}\tag{2}$$

in which $\boldsymbol{\Theta}$ is a diagonal matrix, indicating that after conditioning on all causes the variables are independent, \mathbf{B} is a square matrix with zeros on the diagonal of causal effects between observed variables, and \mathbf{A} is a factor-loading matrix. The variance–covariance matrix of $\boldsymbol{\eta}_C$ may in turn be modeled in various ways to achieve complicated model setups. The expression above is well-known in structural equation modeling (SEM; Kaplan 2000; Wright 1921), which allows for confirmatory testing of causal models.

Suppose there are no unobserved causes to any of the variables in \mathbf{y}_C , and the variables in \mathbf{y}_C are only caused by other variables in \mathbf{y}_C . The corresponding model for $\boldsymbol{\Sigma}$ becomes

$$\boldsymbol{\Sigma} = (\mathbf{I} - \mathbf{B})^{-1} \boldsymbol{\Theta} (\mathbf{I} - \mathbf{B})^{-1\top}.\tag{3}$$

In this expression, \mathbf{B} can now be seen to encode the causal model (Pearl, 2000). Table 1 summarizes the comparison between such causal models and GGMs. Although useful for generating data, we can immediately see several problems in exploratory estimation of \mathbf{B} without any prior knowledge. First, $\boldsymbol{\Sigma}$ contains $n_i(n_i + 1)/2$ elements, $\boldsymbol{\Theta}$ contains n_i parameters, and \mathbf{B} contains $n_i(n_i - 1)$ parameters. As a result, the model above is under-identified without stringent restrictions on \mathbf{B} . One assumption is that \mathbf{y}_C can be ordered such that \mathbf{B} is lower triangular, indicating that if this matrix is used to draw a directed graph—a graph in which $A \rightarrow B$ indicates that A causes B —that graph does not contain

any cycles. Such a graph is called a directed acyclic graph (DAG; Kalisch and Bühlmann 2007; Pearl 2000), meaning that directed edges cannot be traced from any node back to itself (e.g., $A \rightarrow B \rightarrow A$). Although cycles can be identified when exogenous variables are present (Rigdon 1995; a property that will be used below in our discussion of structural vector-autoregression), interpreting such cycles is still not without problems (Hayduk, 2009). Several software packages exist that aim to find such a DAG (e.g., *pcalg*, Kalisch et al. 2012; see also *bnlearn*, Scutari 2010). However, the assumption of acyclicity is debatable in the context of psychological variables (Schmittmann et al., 2013) because many effects can be plausibly assumed cyclic (e.g., fatigue \rightarrow concentration problems \rightarrow stress \rightarrow fatigue).

Second, the same structure for Σ can be obtained under various different specifications of B . Thus, many equivalent models can lead to exactly the same fit. This can be seen because several matrix decompositions of Σ , such as a Cholesky decomposition or an eigendecomposition, can be used to produce equivalently fitting B . The problem of equivalent models is also well-known in the literature on directed networks and SEM (MacCallum et al., 1993; Pearl, 2000). For example, the following three causal models are not statistically distinguishable:

1. Concentration \rightarrow Fatigue \rightarrow Insomnia
2. Concentration \leftarrow Fatigue \rightarrow Insomnia
3. Concentration \leftarrow Fatigue \leftarrow Insomnia

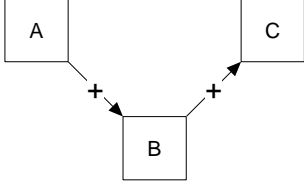
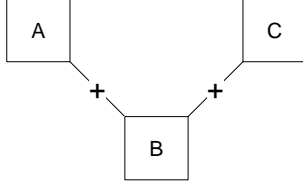
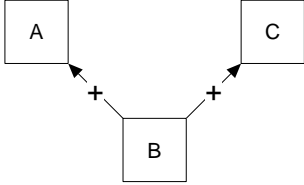
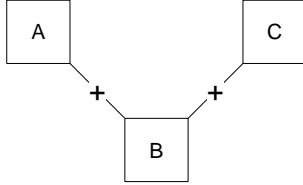
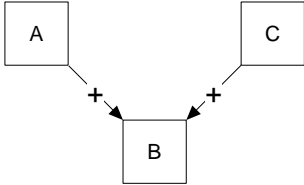
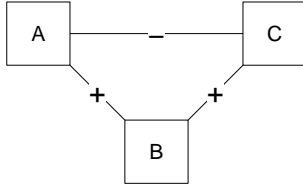
All three models only imply that concentration and insomnia are conditionally independent given fatigue. With more variables, the number of potential equivalent models increases drastically, making it evident that model search is likely to fail. Although exploratory search algorithms exist that attempt to identify such causal models (e.g., Kalisch et al. 2012), these algorithms rely on the assumption of acyclicity and, in our experience, rarely result in interpretable models. With exogenous predictors, causal models become more easily identified, but edges are often still estimated to be in the wrong direction (see our discussion on structural VAR below).

Third, exploratory search of causal networks critically relies on the assumption that no latent variables caused some of the covariation in the dataset. For example, suppose a single common cause was responsible for all covariation between observed variables. Conditioning on none of the observed variables would lead to independence; thus, every fully connected DAG would fit the data equally well (which is a saturated model). Every one of these fully connected DAGs comes with strong causal hypotheses; all of them are wrong.

We consider equivalent models, estimation errors in direction of effect, and the reliance on no latent variables to be considerable downsides to using causal networks or DAGs in the discovery of potential psychological dynamics because the added direction of effect comes with a strong causal hypothesis on what would happen under intervention. To this end, we prefer the undirected GGM, which is saturated rather than overidentified (if all edges are present), does not feature equivalent models, does not suffer from a cumbersome direction of causal effect, does not require the assumption of acyclicity, and is easily parameterized using partial correlation coefficients (Epskamp et al., 2016c). In the presence of latent variables, the GGM also shows a fully connected cluster of nodes. However, edges in this cluster do

Table 1

Overview of Causal Models (Directed Networks) and Gaussian Graphical Models (Undirected Networks)

	Causal model	Gaussian graphical model
$\Sigma^{-1} =$	$(I - B)^{\top} \Theta^{-1} (I - B) =$	K
$A \perp\!\!\!\perp C \mid B$		
$A \perp\!\!\!\perp C \mid B$		
$A \not\perp\!\!\!\perp C \mid B$		
R packages (confirmatory)	Any SEM package	<i>lvnet</i> (fit measures); <i>qgraph</i> (fit measures); <i>ggm</i> (estimation only); <i>glasso</i> (estimation only)
R packages (exploratory)	<i>pcalg</i> ; <i>bnlearn</i>	<i>qgraph</i> (EBICglasso function); <i>glasso</i> (no automatic tuning parameter selection); <i>huge</i> ; <i>parcor</i> ; <i>BDgraph</i> ; <i>lvnet</i> (for GGM at latent or residual level of SEM)
Pros	Causal interpretation; allows for confirmatory testing of causal hypotheses	No equivalent models; fast structure and parameter estimation using LASSO; edges parametrizable as partial correlation coefficients; edges interpretable as predictive effects; latent variables result in clusters; edges can be indicative of potential causal effects
Cons	Exploratory estimation requires assumption of acyclicity; many equivalent models; direction of effect poorly or not identified; strongly depends on assumption of no latent variables	No direction of effect; collider structure can induce spurious edge; LASSO estimation assumes true model is sparse

not impose causal direction. Thus, the GGM gives insight into potential latent variables through its clustering and is already being used in psychometrics as an extra tool in factor analysis (e.g., Golino and Epskamp 2016).

To investigate the structure of a GGM under the causal model of Equation (3), in which observed variables can only be caused by other observed variables, we can invert that expression to obtain

$$\mathbf{K} = (\mathbf{I} - \mathbf{B})^\top \boldsymbol{\Theta}^{-1} (\mathbf{I} - \mathbf{B}), \quad (4)$$

in which $\boldsymbol{\Theta}^{-1}$ is still a diagonal matrix. It becomes evident that there is no longer a matrix inversion needed and that the sparsity in \mathbf{B} directly corresponds to the sparsity in \mathbf{K} . We can derived that κ_{ij} equals zero if there is no directed edge between node i and j (e.g., $Y_i \rightarrow Y_j$ or $Y_i \leftarrow Y_j$) and if there is no common effect of node i and node j (e.g., $Y_i \rightarrow Y_k \leftarrow Y_j$; Koller and Friedman 2009). Thus, under the causal model of Equation (3), a link in a GGM emerges as a result of a causal link or due to a common effect. Therefore, the GGM can highlight the backbone of the causal structure, and links in the GGM can be indicative of potential causal effects.

The Gaussian Graphical Model and Multiple Regression

An edge in a GGM indicates that one node predicts a connected node after controlling for all other nodes in the network. This can also be shown in the relationship between coefficients obtained from least-squares prediction and the inverse variance–covariance matrix. Let $\mathbf{\Gamma}$ represent an $n_i \times n_i$ matrix with zeros on the diagonal. Each row of $\mathbf{\Gamma}$, without the diagonal element $\mathbf{\Gamma}_{i,-(i)}$, contains the regression coefficients obtained in a multiple regression model:⁶

$$y_{ci} = \tau + \mathbf{\Gamma}_{i,-(i)} \mathbf{y}_{c,-(i)} + \varepsilon_{ci}. \quad (5)$$

As such, γ_{ij} encodes how well the j th variable predicts the i th variable. This predictive effect is naturally symmetric; if knowing someone’s level of insomnia predicts his or her level of fatigue, then conversely knowing someone’s level of fatigue allows us to predict his or her level of insomnia. As a result, γ_{ij} is proportional to γ_{ji} . There is a direct relationship between these regression coefficients and the inverse variance–covariance matrix (Meinshausen and Bühlmann, 2006). Let \mathbf{D} denote a diagonal matrix on which the i th diagonal element is the inverse of the i th residual variance: $d_{ii} = 1/\text{Var}(\varepsilon_{Ci})$. As a result, it can be shown (Pourahmadi, 2011) that

$$\mathbf{K} = \mathbf{D} (\mathbf{I} - \mathbf{\Gamma}). \quad (6)$$

Thus, κ_{ij} is proportional to γ_{ij} . A zero in the inverse variance–covariance matrix indicates that one variable does not predict another. Consequently, the network tells us something about the extent to which variables predict each other. In the case of Figure 1, the network demonstrates that insomnia and fatigue, as well as fatigue and concentration, predict each other. This does not mean that knowing someone’s level of insomnia does not say anything about that person’s concentration problems—because these nodes are connected via an indirect path, they may correlate with each other—but merely that fatigue mediates this

⁶This expression should not be confused with Equation 2, which we used as generating model. Here, we do not assume error terms are independent and obtain $\mathbf{\Gamma}_{i,-(i)}$ by univariate multiple regressions.

predictive effect. When someone’s level of fatigue is known, also knowing that person’s level of insomnia does not add any predictive value to that person’s ability to concentrate.

Undirected Networks as a Causal Model

The network structure found in a GGM can be interpreted as showing genuine mutual causation between two nodes of the network—manipulating one node can affect the other and vice versa. Mathematically, the GGM can be shown to have the same form as the Ising model from statistical physics (Epskamp et al., 2010; Ising, 1925), except that the Ising model only models binary data and therefore has a different normalizing constant. This is because both models are part of a class of models called pairwise Markov random fields (Lauritzen, 1996; Murphy, 2012), which have been extensively used to model complex behavior in physical systems. For example, the Ising model uses nodes to represent particles and edges to represent the distance between particles. Particles, in essence very small magnets, are then modeled to have their north pole face up or down. Particles tend to orient themselves randomly at normal temperatures but align at low temperatures. Because particles tend to align at low temperatures, one particle being aligned causes an adjacent particle to align in that same way and vice versa. These relationships are naturally symmetric (Epskamp et al., 2010). By applying the analogy of the Ising model for particles to the GGM shown in Figure 1, we could say that these symptoms tend to be in the same state (of alignment) if there is a positive connection between them and if they tend to be in different states—as long as there is a negative connection. In this system, suffering from insomnia could lead a person to also suffer from fatigue and experience concentration problems (Epskamp et al., 2010; van Borkulo et al., 2014).

Estimation

A GGM can be estimated in datasets where cases can be assumed to be independent. Two common examples of such data are cross-sectional data, in which every subject is only measured once on a set of response items, or $n = 1$ time-series data that feature large intervals between measurement occasions. In time-series data featuring shorter intervals, a GGM can be estimated as well; in this case, the network could be termed a contemporaneous network. However, as we argue in the next section on temporally ordered data, better methods exist that take temporal information into account in addition to modeling the contemporaneous effects of a GGM. In cross-sectional data analysis, only one observation per subject is available; thus, we cannot expect to estimate subject-specific means or GGM networks. It is typically assumed that the cases all share the same distribution. That is,

$$\mathbf{y}_P \sim N(\mathbf{0}, \mathbf{\Sigma}), \quad (7)$$

in which \mathbf{y}_P denotes the random response of subject P . Similarly, in $n = 1$ time-series data we can make a similar assumption:

$$\mathbf{y}_T \sim N(\mathbf{0}, \mathbf{\Sigma}),$$

in which \mathbf{y}_T denotes the random response of a subject on all items at time point T . In both cases, the full likelihood can be readily obtained, and the variance–covariance matrix $\mathbf{\Sigma}$ can reliably be estimated using MLE, least-squares estimation, or Bayesian estimation.

The maximum likelihood solution of \mathbf{K} —the precision matrix encoding a GGM—can be obtained by standardizing the inverse sample variance–covariance matrix and by multiplying all off-diagonal elements by -1 . To obtain a sparse network (i.e., \mathbf{K} contains zeros), model search can be performed by iteratively adding and removing edges and fitting confirmatory GGMs. In recent literature, it has become increasingly popular to use regularization techniques, such as penalized MLE, to jointly estimate model structure and parameter values (Costantini et al., 2015; van Borkulo et al., 2014). The *least absolute shrinkage and selection operator* (LASSO; Tibshirani 1996) has been shown to perform well in quickly estimating model structure and parameter estimates of a sparse GGM (Friedman et al., 2008; Meinshausen and Bühlmann, 2006; Yuan and Lin, 2007). A particularly fast variant of LASSO is the *graphical LASSO* (glasso; Friedman et al. 2008), which directly penalizes elements of the inverse variance–covariance matrix (Witten et al., 2011; Yuan and Lin, 2007). LASSO utilizes a tuning parameter which can be chosen in a way that optimizes cross-validated prediction accuracy or that minimizes information criteria such as the extended Bayesian information criterion (EBIC; Chen and Chen 2008). Estimating a GGM with the glasso algorithm in combination with EBIC model selection has been shown to work well in retrieving the true network structure (Epskamp, 2016; Foygel and Drton, 2010) and is currently the dominant method for estimating the GGM in psychological data (see Epskamp and Fried 2016 for an introduction to this methodology aimed at empirical researchers).

Several software packages allow for GGM estimation as described above. Maximum likelihood estimation can be performed by inverting and standardizing the sample variance–covariance matrix, which can be done in any programming language and in many statistical programs. In the open-source statistical programming language R (R Core Team, 2016), automated procedures have been implemented in the *corpcor* package (Schäfer et al., 2015) or the *qgraph* (Epskamp et al., 2012) package. The *qgraph* package also supports thresholding via significance testing or false discovery rates. The glasso algorithm is implemented in the *glasso* (Friedman et al., 2014) and *huge* (Zhao et al., 2015) packages. The *huge* package also allows for selection of the tuning parameter using cross validation or EBIC. The EBIC-based tuning parameter selection alongside the glasso package, using only a variance–covariance matrix as input, has been implemented in the *qgraph* package. The *parcor* package (Krämer et al., 2009) implements other LASSO variants to estimate the GGM. The *BDgraph* package (Mohammadi and Wit, 2015) implements a Bayesian method to estimate the undirected structure. Finally, fitting an estimated GGM to data can be done in the R packages *ggm* (Marchetti et al., 2015) and *lwnet* (Epskamp et al., 2016c).

Cross-Sectional Data and Between-Subjects Effects

A type of data to which the GGM is now often applied is data belonging to multiple subjects that are all measured only once (e.g., Isvoranu et al. 2016b; van Borkulo et al. 2015). Such a dataset is often termed cross-sectional data, and such an analysis is often termed a between-subjects analysis. However, the term between-subjects analysis might often not be warranted, as it is difficult to distinguish between variance due to short-term variation of the average (within-person effects) and the variation of the mean (between-person effects) using only cross-sectional data (Hamaker, 2012). It is well known that subjects might respond differently when measured multiple times (Lord et al., 1968). As such, the single

observation per subject leads to the time point and the subject being random: $\mathbf{y}_{[T,P]}$. We might make the argument that two distinct sources of variation cause the outcome. Because measurements are nested in people, we need to model such a separation with a chain (Bolger and Laurenceau, 2013):

$$\begin{aligned}\mathbf{y}_{[T,P]} &\sim N(\boldsymbol{\mu}_p, \boldsymbol{\Theta}_p) \\ \boldsymbol{\mu}_p &\sim N(\mathbf{0}, \boldsymbol{\Omega}),\end{aligned}$$

in which we can assume, without loss of information, an overall mean of $\mathbf{0}$. We can invert and standardize variance-covariance matrix $\boldsymbol{\Omega}$ to obtain a GGM:

$$\mathbf{K}^{(\boldsymbol{\Omega})} = \boldsymbol{\Omega}^{-1}.$$

We call this a between-subjects network. The matrix $\boldsymbol{\Theta}_p$ can also be inverted and standardized to a GGM to obtain a within-person network:

$$\mathbf{K}_p^{(\boldsymbol{\Theta})} = \boldsymbol{\Theta}_p^{-1}.$$

Section 4 of the supplementary materials show that such a zero-order network is actually a mixture of temporal and contemporaneous effects. Without temporally ordered data, temporal effects might also lead to edges in this within-person network. Therefore, we will term this network a *within-subjects network* and show below how temporally ordered data can separate these effects into a contemporaneous and temporal network.

It is immediately clear that subject-specific variance-covariance matrix $\boldsymbol{\Theta}_p$ (and as a result the GGM) cannot be estimated from a single set of responses. Moreover, even if we assume that within-person effects are equal across subjects and drop the subscript p , this still leaves us without an estimable model because $\boldsymbol{\mu}$ is also assumed to be normally distributed. Therefore, in no way do we know if deviations from the grand mean are due to the within-person variance in $\boldsymbol{\Theta}$ or the between-person variance in $\boldsymbol{\Omega}$. Writing $\boldsymbol{\varepsilon}_{[t,p]} = \mathbf{y}_{[t,p]} - \boldsymbol{\mu}_p$, the GGM estimated on such data becomes

$$\mathbf{K} = \left(\boldsymbol{\Theta} + \boldsymbol{\Omega} + 2\text{Cov}(\boldsymbol{\varepsilon}_{[T,P]}, \boldsymbol{\mu}_P) \right)^{-1},$$

which is not a simple function of the between-subjects GGM and the contemporaneous GGM even when the covariance $2\text{Cov}(\boldsymbol{\varepsilon}_{[T,P]}, \boldsymbol{\mu}_P)$ is assumed to be zero. Only when no short-term within-person variation, $\boldsymbol{\Theta} = \mathbf{O}$, or no between-subjects variation, $\boldsymbol{\Omega} = \mathbf{O}$, is assumed does the cross-sectional GGM correspond exactly to one of the two networks.

This is not to say that cross-sectional data analysis is wrong. Many groundbreaking scientific findings have been obtained through cross-sectional data analysis (e.g., smoking leads to lung-cancer), but it simply cannot disentangle between-subjects relationships from short term within-subjects relationships (Hamaker, 2012). For example, cross-sectional analysis cannot distinguish whether or not fatigue and concentration correlate because whenever people feel fatigued they also concentrate poorly or because people who are on average fatigued also tend to concentrate poorly on average. We conducted a simulation study to assess the performance of a cross-sectional GGM estimation, where we generated data on completely different within- and between-subjects networks. The results are

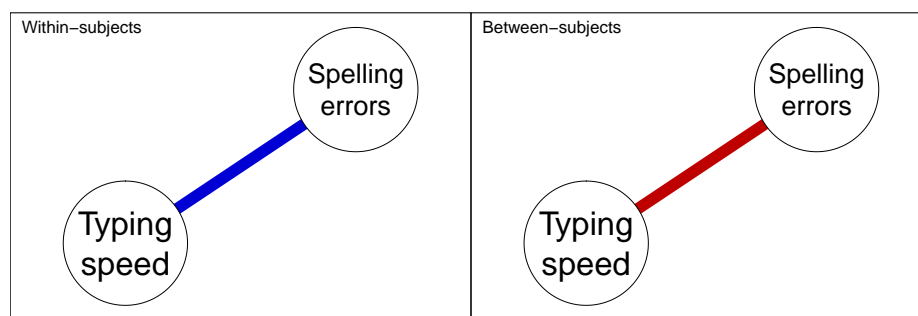
reported in Section 1.1 of the supplementary materials and show that the resulting cross-sectional GGM generally does not contain edges that are not present in either the within- or between-subjects network. Depending on the relative within-to-between person variance, the cross-sectional analysis will pick up the within-person network, the between-person network, or a mixture of the two. Section 1.1 furthermore shows that if two observations per person are analyzed (rather than just one), estimating a GGM on within-subjects centered pooled data adequately captures the within-subjects network (assuming it is the same for every subject), and that a GGM estimated on the subject-specific means can estimate the between-subjects networks.

Cross-sectional analysis offers powerful exploratory insights into datasets and can also lead to the generation of hypotheses pertaining to psychological dynamics. An important consideration is that a typical cross-sectional questionnaire or interview is vastly different than a typical ESM questionnaire, and many cross-sectional studies aim to measure variables that are more stable over time and for which a time-series analysis might not make sense. Good examples of this are recent network analyses in the area of schizophrenia (Isvoranu et al., 2016a,b), in which the impact of environmental factors (e.g., childhood trauma, urbanization) on psychotic symptoms and general psychopathology was studied. Such variables do not vary much over time; therefore, a cross-sectional analysis seems more suitable here. Other examples are questionnaires asking participants to rate symptoms over a period of several weeks or to describe themselves as “I am a person who. . .” In such cases, the cross-sectional network can be interpreted as a between-subjects network, which, as we argue below, can also be indicative of potential causal pathways.

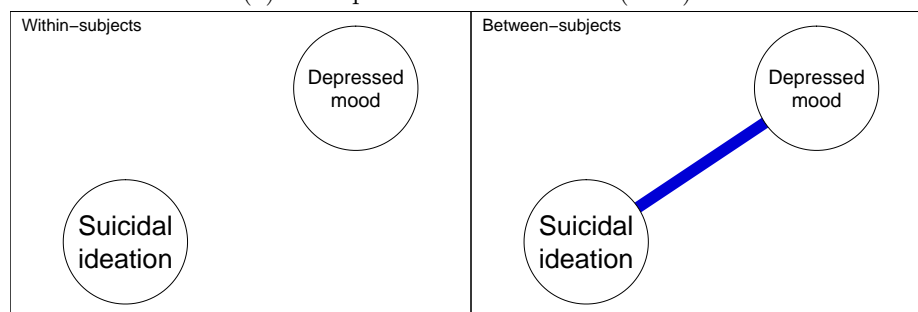
Causation at the Between-Subjects Level

Although a single response cannot separate the stationary mean from deviations of that mean for a particular subject, the same argument can be made for the mean μ_P , which could be a mixture between long-term averages (e.g., years) and deviations from an average in the period of that study (e.g., the average effect in a period of two weeks in which ESM data is gathered). Here, we interpret the stationary means as being locally stationary: the average of a subject in a relatively short time span of measurement (e.g., a few weeks). As such, we do not interpret the mean vector μ_P as a lifetime average. Instead, we assume it could change, potentially due to experimental intervention. As a result, we argue that the between-subjects network can also be indicative of potential causal pathways—regardless of whether it is estimated from a cross-sectional interview concerning variables that are not expected to vary much over time or obtained from estimating the means from time-series data.

Hamaker (2012) described an example of how within- and between-person effects can strongly differ from each other. Suppose we let people write several texts, and we measure the number of spelling errors they make and the number of words per minute they type (typing speed). We would expect to see the seemingly paradoxical network structures shown in Figure 2, Panel (a). We would also expect a positive relationship in the contemporaneous network. When a person types faster than his or her average typing speed, that person will make more spelling errors. Conversely, we would expect a negative relationship in the between-person network (e.g., people who type fast, on average, generally make fewer spelling errors). This is because people who type fast, on average, are likely to be more



(a) Example based on Hamaker (2012).



(b) Hypothetical example of patients with little within-subject variation but strong individual differences.

Figure 2. Two hypothetical examples of differing within- and between-person networks. The networks on the left indicates the within-person network, showing that personal deviations from the means predict each other at the same time point, and the networks on the right indicates the between-subjects network, showing how the *means* of different subjects relate to one another.

skilled in writing (e.g., a courtroom stenographer) and are less likely to make a lot of spelling errors, compared to someone who types infrequently. Panel (b) of Figure 2 shows another hypothetical example in which the structures might differ. Suppose we measure two groups of subjects over time, one group in which subjects always scores high on “depressed mood” and “suicidal ideation” and another group in which subjects always score low on both symptoms. Suppose that these subjects do not score correlated deviations from their means, the only present correlation then would appear in the between-subjects network (this is a hypothetical example, often both networks will show an edge).

The different ways of thinking about the effects of manipulations in time-series models can be organized in terms recently developed from interventionist accounts of causation (Woodward, 2005). According to Woodward, causation is fleshed out in terms of interventions: X is a cause of Y if an intervention (natural or experimental) on X leads to a change in Y . Statistically, the interventionist account is compatible with, for example, Pearl’s 2000 semantics in terms of a “do-operator.” Here, an intervention on X is represented as $\text{Do}(X = x)$, and the causal effect on Y is formally expressed as $\mathbb{E}(Y \mid \text{Do}(X = x))$. Pearl distinguished this from the classical statistical association, in which no intervention is present, and we get the ordinary regression $\mathbb{E}(Y \mid \text{See}(X = x))$. This is a useful notation because it immediately raises the important point that there is a difference between

doing and seeing, which of course parallels the classic distinction between experimental and correlational research (Cronbach and Meehl, 1955).

Cashing out causal effects in terms of interventions is useful to understand the intervention $\text{Do}(X = x)$. We can think of this in terms of a random shock to the system, which sets X to value x at a particular time point and evaluates the effect on another variable Y on the next time point (or series of time points as in continuous time models). If we want to gauge this type of causal relationship, we might look at the within-subjects VAR model. Consider Hamaker’s 2014 example regarding typing errors: If a researcher forced a person to type very fast, that researcher would need to evaluate the within-person data, which would show a positive association between typing speed and the number of errors. In this example, between-subjects data would be misleading because individual differences would probably yield a negative correlation between speed and accuracy—faster typists are more likely to make less errors.

However, we can also think of a manipulation that sets X to value x in a different way, for instance, by inducing a long-term change in the system that leads it to converge on $X = x$ in expectation. To evaluate the effect of this type of intervention, it is important to consider the behavior of the system as it relates to the changes of the intercept of X . Clearly, in order to evaluate this type of intervention, the within-subjects time-series model is useless (because of stationarity). However, the between-subjects model may contain important clues because it contains the relationships between the long-term averages across people. Thus, if we want to gauge the effect of a long-term change (most plausibly conceptualized as a change in intercept), the between-subjects model is a better guide. In terms of Panel (b) of Figure 2, if we are interested in the effect of changing someone structurally—treating a patient to experience lower suicidal ideation on average—our preferred source of causal hypothesis generation would likely stem from the between-subjects model.

Many such examples can be envisioned, especially in the field of psychopathology. For instance, short-term deviations from the mean in abusing a substance might not immediately develop tolerance or lead to one suffering from work or life inferences, but a subject who abuses a substance on average over a long time period might develop these problems (example based on variables used by Rhemtulla et al. 2016). A between-subjects network could similarly show that loneliness mediates the effect of losing a spouse on depressive symptoms (Fried et al., 2015) or highlight the possible effects of childhood trauma and urbanization on psychotic symptoms (Isvoranu et al., 2016a,b)—both cases in which within-subject networks based on short-term deviations from the average seem less applicable.

Empirical Example 1: Personality Inventory Items

Figure 3 shows an example of a GGM estimated using glasso in combination with EBIC model selection. This network was estimated on the `bfi` dataset from the *psych* R package (Revelle, 2010). The dataset contains the responses of 2,800 people on 25 items designed to measure the Big Five personality traits (Goldberg, 1993; McCrae and Costa, 1997). The network shows many meaningful connections, such as “am indifferent to the feelings of others” being linked to “inquire about others’ well-being,” “don’t talk a lot” being linked to “find it difficult to approach others,” and “carry the conversation to a

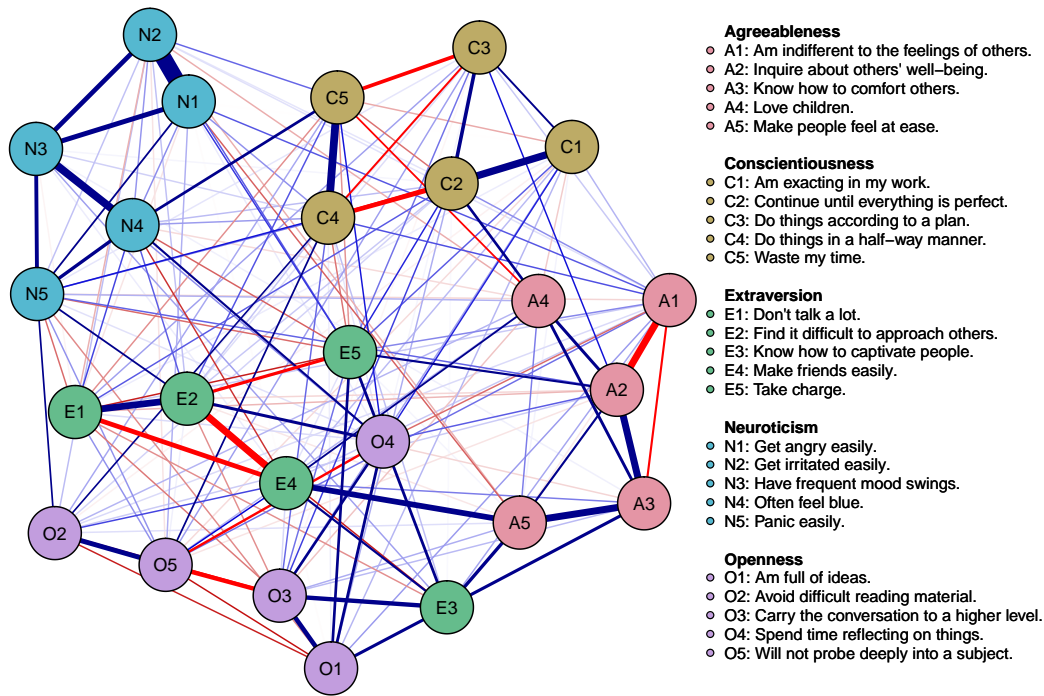


Figure 3. An example of a network model estimated on the BFI personality dataset from the psych package in R (cross-sectional data, $n = 2,800$). Nodes represent variables (in this case personality inventory items), and edges between the nodes represent partial correlation coefficients. The network was estimated using the glasso in combination with EBIC model selection, using the EBICglasso function in the *qgraph* package.

higher level” being linked to “know how to captivate people.” For a detailed discussion on the interpretation of such models in personality research, see Costantini et al. (2015).

Temporally Ordered Data

In line with a call for more intraindividual and person-based research (Molenaar, 2004), an increasingly popular form of data pertains to $n = 1$ time series, in which a single individual is measured repeatedly over a period of time. One such situation is in clinical practice (Epskamp et al., tted), where a patient can be measured several times per day over a period of a few weeks. We will limit our discussion to data obtained in a relatively short time-frame so that we can reasonably assume the model will remain stable over time. Then, we can apply the methodology above to obtain a GGM for the $n = 1$ data. However, such an analysis does not take temporal ordering of data into account (i.e., relationships between measurement occasions) and only investigates contemporaneous relationships between variables (e.g., within the same measurement occasion). This is important for several reasons. First, valuable information, especially in the context of discovering psychological

dynamics, might be contained at the temporal level rather than at the contemporaneous level. Temporal prediction is termed *Granger causality* in the economic literature (Eichler, 2007; Granger, 1969), and it satisfies at least the temporal requirement for causation (i.e., the cause must precede the effect). Second, although we argue that contemporaneous effects are also insightful in exploratory analysis, not taking temporal ordering into account might bias the estimated contemporaneous relationships (see Section 4 of the supplementary materials). For example, if one variable causes itself and another variable at the next time, then not taking temporal ordering into account turns that variable into a latent cause, which would produce an edge in the GGM. Third, temporal information is needed when constructing the joint likelihood over time (e.g., to obtain the information retained in a system over time; Epskamp 2017a; Quax et al. 2013).

The simplest way to deal with temporal ordering of cases is to incorporate the effect between consecutive measurements (Shumway and Stoffer, 2010; Hamilton, 1994; Chatfield, 2016). This is called a Lag-1 model because it includes both measurements at the current time point t as well as measurements from the previous time point $t - 1$. We will focus our discussion on Lag-1 models, noting that everything below also generalizes to more complicated models. In intraindividual analysis, VAR (Brandt and Williams 2007; Rosmalen et al. 2012) has gained substantive footing in visualizing temporal information through networks (e.g., Bringmann et al. 2013, 2015; Wigman et al. 2015). These analyses mostly only focus on temporal effects and do not model the contemporaneous relationships.

We can combine current and lagged measurements in a single vector $\mathbf{y}_{\{t-1,t\}}^\top = \begin{bmatrix} \mathbf{y}_{t-1}^\top & \mathbf{y}_t^\top \end{bmatrix}$ and form a general modeling framework:

$$\mathbf{y}_{\{t-1,t\}} = \mathbf{B}\mathbf{y}_{\{t-1,t\}} + \boldsymbol{\varepsilon}_{\{t-1,t\}}, \quad (8)$$

in which \mathbf{y}_{t-1} are treated as exogenous; thus, \mathbf{B} does not contain any effects towards any of the lagged variables,

$$\mathbf{B} = \begin{bmatrix} \mathbf{O} & \mathbf{O} \\ \mathbf{B}_{21} & \mathbf{B}_{22} \end{bmatrix},$$

and $\boldsymbol{\varepsilon}$ is distributed normally,

$$\boldsymbol{\varepsilon}_{\{T-1,T\}} \sim N(\mathbf{0}, \boldsymbol{\Theta}).$$

We do not set $\boldsymbol{\Theta}$ to be diagonal but instead model its inverse as a GGM, which we can arbitrarily separate into four blocks:

$$\boldsymbol{\Theta}^{-1} = \mathbf{K}^{(\boldsymbol{\Theta})} = \begin{bmatrix} \mathbf{K}_{11}^{(\boldsymbol{\Theta})} & \mathbf{K}_{12}^{(\boldsymbol{\Theta})} \\ \mathbf{K}_{21}^{(\boldsymbol{\Theta})} & \mathbf{K}_{22}^{(\boldsymbol{\Theta})} \end{bmatrix}.$$

It is clear that every generating model, as seen in Equation (2), can be represented in this framework, where covariation between exogenous or latent variables can be represented in the variance-covariance structure of the residuals. However, we argue, and show in the simulations shown in section 1.2 of the supplementary materials, that due to model equivalences, structuring the GGM of the residuals can still give insight into potential causal relationships between observed variables. Using this framework, we can construct several modeling frameworks that allow us to jointly model temporal and contemporaneous effects

in a sparse manner. Such effects can then be summarized in two network models: the temporal network, which is a directed network indicating temporal prediction or Granger causality, and the contemporaneous network, which is either a directed or undirected network of effects in the same window of measurement.

First, using *structural VAR* (Chen et al. 2011a), also called *unified SEM* (Gates et al. 2010), we specify

$$\mathbf{B} = \begin{bmatrix} \mathbf{O} & \mathbf{O} \\ \mathbf{B}_{21} & \mathbf{B}_{22} \end{bmatrix},$$

and

$$\boldsymbol{\Theta}^{-1} = \mathbf{K}^{(\boldsymbol{\Theta})} = \begin{bmatrix} \mathbf{K}_{11}^{(\boldsymbol{\Theta})} & \mathbf{O} \\ \mathbf{O} & \mathbf{K}_{22}^{(\boldsymbol{\Theta})} \end{bmatrix},$$

in which we keep $\mathbf{K}_{11}^{(\boldsymbol{\Theta})}$ saturated and force $\mathbf{K}_{22}^{(\boldsymbol{\Theta})}$ to be diagonal.⁷ To identify the model, we include all diagonal elements of \mathbf{B}_{21} (autoregressions). Model selection can be used to structure temporal effects in \mathbf{B}_{21} and contemporaneous effects in \mathbf{B}_{22} .

Second, the conditional distribution of \mathbf{y}_T given $\mathbf{y}_{[T-1,]} = \mathbf{y}_{t-1}$ can be modeled as a GGM. Doing so is equivalent to modeling the residual structure of a regular VAR model as a GGM. This is called a graphical VAR (Wild et al., 2010). We obtain the graphical VAR model by setting

$$\mathbf{B} = \begin{bmatrix} \mathbf{O} & \mathbf{O} \\ \mathbf{B}_{21} & \mathbf{O} \end{bmatrix}$$

and

$$\boldsymbol{\Theta}^{-1} = \mathbf{K}^{(\boldsymbol{\Theta})} = \begin{bmatrix} \mathbf{K}_{11}^{(\boldsymbol{\Theta})} & \mathbf{O} \\ \mathbf{O} & \mathbf{K}_{22}^{(\boldsymbol{\Theta})} \end{bmatrix},$$

in which we keep $\mathbf{K}_{11}^{(\boldsymbol{\Theta})}$ saturated and perform model selection on temporal effects in \mathbf{B}_{21} and contemporaneous effects in $\mathbf{K}_{22}^{(\boldsymbol{\Theta})}$. It can be seen that when $\mathbf{B}_{21} = \mathbf{O}$, the graphical VAR model is exactly the same as the GGM model described above for independent cases. Thus, the graphical VAR model can be seen as a generalization of the GGM model to temporally ordered data. Graphical VAR only differs from regular VAR in that the contemporaneous structure is modeled and represented as a GGM, instead of being saturated. This leads to a strikingly different interpretation of the VAR model; the VAR model can be seen as an inclusion of temporal effects on a GGM.

A third and unexplored option is to simply fit a GGM to the Toeplitz matrix (joint variance–covariance matrix of current and lagged variables). We can term this framework a *Toeplitz GGM*. That is, we set $\mathbf{B} = \mathbf{O}$ and model all elements of $\mathbf{K}^{(\boldsymbol{\Theta})}$. We can force a search algorithm to not set elements in exogenous variance–covariance matrix $\mathbf{K}_{11}^{(\boldsymbol{\Theta})}$ to zero (e.g., in LASSO regularization we can opt to estimate these elements unregularized). This model straightforwardly estimates using the glasso algorithm and can be used on relatively high-dimensional datasets. The contemporaneous network can be shown to be the same as in graphical VAR, but the temporal network differs from that of structural VAR and graphical VAR. Edges in the temporal network obtained via a Toeplitz GGM can be spurious due

⁷In structural VAR, we specify $\boldsymbol{\Theta}^{-1}$ to be block diagonal. As a result, its inverse (the residual variance–covariance matrix) is also block diagonal.

to a common effect between a node at $t - 1$ and a node at t . For example, when A_{t-1} causes A_t , and B_t causes A_t at the contemporaneous time level, a temporal edge is induced between A_{t-1} and B_t . Because conditioning on time point t can induce edges between time point $t - 1$ and t , the interpretation of the temporal network becomes difficult. For this reason, we focus our discussion on structural VAR and graphical VAR and only note that a Toeplitz GGM poses a potential third option for large datasets where estimation and model selection of structural VAR and graphical VAR might be challenging.

Section 2 of the supplementary materials shows that the structural VAR and graphical VAR models are equivalent, and estimating one model can lead to an equivalent conceptualization in the other framework. Table 2 summarizes this information. The contemporaneous structure of the graphical VAR model is the GGM equivalent to the directed network in structural VAR. If data are generated via a structural VAR model, the corresponding contemporaneous network in the graphical VAR model will feature an edge whenever there is an edge between two variables in the contemporaneous network of the structural VAR model or whenever there is a common effect between two variables in the contemporaneous network of the structural VAR model. Thus, the contemporaneous GGM in graphical VAR offers similar exploratory insight into potential causal effects at a contemporaneous time level as described in our discussion of the GGM above. The temporal structure between graphical VAR and structural VAR differs in that in graphical VAR mediators at the contemporaneous time level are not taken into account in the estimation of the temporal model. As Table 2 shows, if A predicts itself over time, and A predicts B in the same measurement occasion, then A predicts B over time as well. Such a mediator is controlled for in structural VAR but not in graphical VAR. This is not necessarily a problem because the temporal network in graphical VAR shows the predictive effects over time and is, therefore, optimal for forecasting. Furthermore, an argument can be made that a researcher might not want to control for contemporaneous effects when estimating temporal effects—that researcher might not want an effect between the present (t) and the future $t + 1$ to be influenced by conditioning on the future.

We performed a simulation study to assess the performance of model selection in structural VAR and graphical VAR, which is reported in Section 1.2 of the supplementary materials. These simulations show that even though the direction of contemporaneous causal effects can be identified, structural VAR often estimates a contemporaneous edge in the wrong direction (e.g., $A \leftarrow B$ instead of $A \rightarrow B$), which induces a wrong hypothesis on a potential causal effect. Graphical VAR does not have this problem and often features undirected edges when there were causal effects in the simulated model but no edge otherwise.

Causation at the Contemporaneous Level

As described above, in order to disentangle temporal and contemporaneous relationships, it is best not to combine them into a single GGM model but rather to investigate them separately. The graphical VAR model (Wild et al., 2010) allows for the estimation of a temporal network and a contemporaneous network of partial correlation coefficients. Both network structures can highlight potential causal pathways. In psychology, there will likely be many causal relationships that occur much faster than the lag interval in a typical ESM study; in which case, these pathways will be captured in the contemporaneous network.

Table 2
Overview of Two Different Methods for Modeling Temporal and Contemporaneous Effects in Time-Series Data

	Structural VAR	Graphical VAR
Example		
Model	$\mathbf{K}^{(\Theta)}$ set to be diagonal	$\mathbf{B}_{21} = \mathbf{O}$, $\mathbf{K}_{12}^{(\Theta)} = \mathbf{O}$ and $\mathbf{K}_{22}^{(\Theta)}$ as GGM
Temporal network	\mathbf{B}_{21}	\mathbf{B}_{21}
Contemporaneous network	\mathbf{B}_{22} (directed)	proportional to $\mathbf{K}_{22}^{(\Theta)}$
Contemporaneous equivalence	$(\mathbf{I} - \mathbf{B}_{22})^\top \mathbf{K}_{22}^{(\Theta)} (\mathbf{I} - \mathbf{B}_{22})$	$\mathbf{K}_{22}^{(\Theta)}$
Temporal equivalence	$(\mathbf{I} - \mathbf{B}_{22})^{-1} \mathbf{B}_{21}$	\mathbf{B}_{21}
Pros	Causally interpretable; allows causal modeling of contemporaneous effects; no potentially spurious connections in temporal network.	Well identified; well defined saturated model; allows sparse modeling of contemporaneous effects; edges indicative of potential causal effects; latent variables result in clusters of undirected edges; temporal network optimal for prediction.
Cons	Potentially poorly identified; model search might lead to reverse directed edges; strong reliance on the assumption of no latent variables; strong interpretation of the direction of effect.	Potentially spurious edges in the temporal network; No direction of effect in contemporaneous network. Limited software for confirmatory estimation.

Note. The dashed line indicates an edge that is present in the graphical VAR model but not in the corresponding structural VAR model.

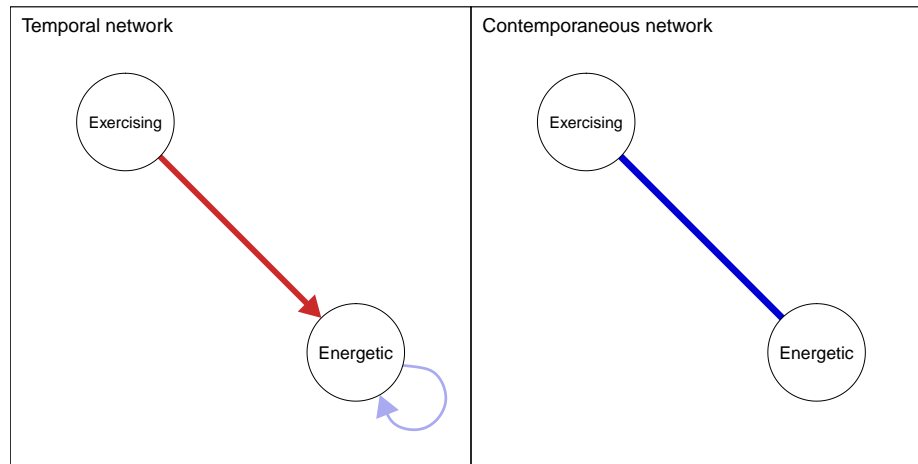


Figure 4. A hypothetical example of two network structures obtained from a graphical VAR analysis. The network on the left indicates the temporal network, demonstrating that a variable predicts another variable at the next time point. The network on the right indicates the contemporaneous network, demonstrating that two variables predict each other at the same time point.

For example, if someone is experiencing bodily discomfort, that will immediately negatively affect that person’s ability to enjoy him or herself (Epskamp et al., tted).

Figure 4 shows a hypothetical example of the two network structures obtained in a graphical VAR analysis and shows how they might plausibly differ. The left panel shows the temporal network. This network shows that whenever the subject in question felt energetic (or tired) this person also felt more (or less) energetic in the next measurement. The temporal network also shows us that after exercising, this person felt less energetic as well. The contemporaneous network in the right panel shows a plausible reverse relationship: Whenever this person exercised, he or she felt more energetic in the same measurement occasion.

Estimation

Graphical VAR and structural VAR can be specified as latent network models (Epskamp et al., 2016c), in which the variance–covariance matrix between latent variables of a SEM model can be modeled as a GGM. Currently only the *lvnet* R package allows for the specification of such models. If a researcher does not want to perform model selection on the residual GGM in graphical VAR, both frameworks can also be specified in any SEM package. The temporal coefficients of the graphical VAR model can also be estimated by multiple regression of all variables on the previous measurement occasion,

$$\mathbf{y}_t = \mathbf{B}_{21}\mathbf{y}_{t-1} + \boldsymbol{\varepsilon}_t,$$

or by estimating univariate models for every variable,

$$y_{ti} = \beta_i \mathbf{y}_t + \varepsilon_{ti},$$

in which β_i denotes the i th row of \mathbf{B}_{21} . The contemporaneous effects can then be obtained by inverting the variance–covariance matrix of the residuals.

Abegaz and Wit (2013) proposed to apply LASSO estimation to jointly estimate the temporal and contemporaneous network structures using the multivariate regression with the covariance estimation (MRCE) algorithm described by Rothman et al. (2010). MRCE involves iteratively optimizing \mathbf{B}_{21} , using cyclical-coordinate descent, and \mathbf{K}_{22} , using the glasso algorithm (Friedman et al., 2008, 2014). EBIC model selection can be used to obtain the best performing model. This methodology has been implemented in two open source R packages: *sparseTSCGM* (Abegaz and Wit, 2015), which aims to estimate the model on repeated multivariate genetic data, and *graphicalVAR* (Epskamp, 2017b), which was designed to estimate the model on the psychological data of a single subject. The *graphicalVAR* package also allows for unregularized multivariate estimation.

Empirical Example 2: Reanalysis of Wichers et al. (2016)

To exemplify the graphical VAR model, we reanalyzed the data from Wichers et al. (2016), which was recently made public by Kossakowski et al. (2017). This dataset consists of 1,478 measurements over the course of 239 days of one patient while he was lowering his antidepressant intake in a double-blind setting. The subject completed, on average, 6.2 items per day and was measured on 50 items. The study was separated into five phases: (1) a baseline period, (2) the period during the experiment before the patient reduced his medication, (3) the period during which the patient reduced his medication, (4) the period during the experiment after the patient reduced his medication, and (5) the period after the experiment. We combined Phase 1 and 2 to obtain four roughly equal-sized groups. Similar to Haslbeck and Waldorp (2016a), who used this data in an empirical example on time-varying temporal VAR network estimation, we selected variables pertaining to the measurement of different mood states. On data from each of the groups, we used the graphicalVAR package to estimate graphical VAR models using the methodology of Abegaz and Wit (2013). We used the MRCE algorithm to perform LASSO regularization on both the contemporaneous and temporal networks. The two tuning parameters (one for the contemporaneous and one for the temporal network) were selected to minimize the EBIC (the EBIC hypertuningparameter γ , which controls the penalization of model complexity, was set to 0.25). We did not regress the first measurement of the day on the last measurement of the previous day, and did not regress measurements on the previous measurement if a measurement in between was missing (e.g., if the “beep” variable indicated 4 and 6, then that would indicate Observation 5 was missing). The networks were standardized as described by Wild et al. (2010).

Figure 5 shows the estimated network structures. It is notable that the temporal networks show very little connections, even though a relatively low value was used for the EBIC tuning parameter γ (to err more on the side of discovery). This seems to suggest that to study the unique dynamics between individual items here we would need to investigate the contemporaneous structure. The contemporaneous networks show more edges in all four periods. Most notable is the presence of two stable clusters of nodes—one includes feeling “satisfied,” “enthusiastic,” “strong,” “cheerful,” and potentially “relaxed,” and another cluster includes feeling “down,” “guilty,” and “lonely.” As described above, such clusters could be indicative of the influence of two latent variables (the connections between the two

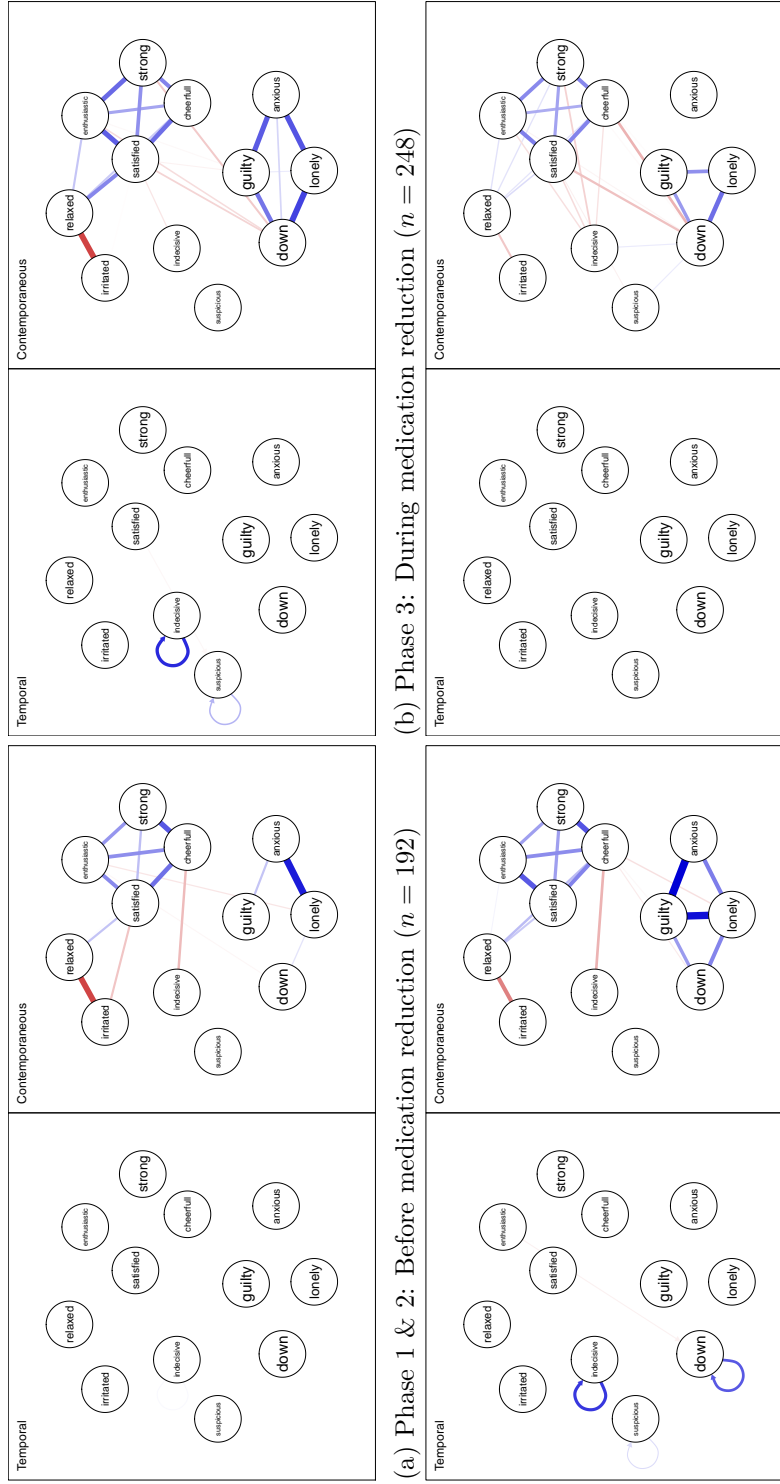


Figure 5. Networks estimated on the different phases of the Wichers et al. (2016) dataset (Kossakowski et al., 2017). Networks were estimated using the *graphicalVAR* package with hypertuning parameter set to 0.25.

clusters are weaker than would be expected from a single latent variable). Furthermore, the negative relationship between feeling relaxed and feeling irritated remains consistently strong, and feeling irritated is mostly disconnected from other nodes. This seems to suggest that feeling relaxed mediates the role between feeling irritated and positive affect items. A possible hypothesis generated here is that feeling relaxed causes both feeling less irritated and feeling more positive affect items. It should be noted that this analysis is highly exploratory and in no way conclusive on such statements. For further reading on this dataset, refer to Wichers et al. (2016) and to Haslbeck and Waldorp (2016a) who estimated a time-varying temporal VAR network as well as a time-varying (i.e., changing structure over time) GGM on this dataset.

Temporally Ordered Data of Multiple Subjects

A type of data that is increasingly common due to the emergence of ESM studies is time series of multiple subjects (e.g., Bringmann et al. 2013, 2015; Möttus et al. 2016; Schmiedek et al. 2010; Wigman et al. 2015). Such datasets pose a promising gateway to study both intraindividual dynamics and between-subjects overlap as well as their differences. Here, we assume that the number of time points might differ per person and that measurement occasions are nested in people. We can model the temporal data of every person with an individual graphical VAR model (dropping subscripts for block matrices used above for notational clarity):

$$\begin{aligned} \mathbf{y}_{[t,p]} &= \boldsymbol{\mu}_p + \mathbf{B}_p (\mathbf{y}_{[t-1,p]} - \boldsymbol{\mu}_p) + \boldsymbol{\varepsilon}_{[t,p]} \\ \boldsymbol{\varepsilon}_{[T,p]} &\sim N(\mathbf{0}, \boldsymbol{\Theta}_p) \\ \boldsymbol{\Theta}_p^{-1} &= \mathbf{K}_p^{(\boldsymbol{\Theta})}, \end{aligned}$$

in which $\boldsymbol{\mu}_p$ indicates the stationary mean vector of subject p (which enters the model because we can no longer assume within-person means are zero without loss of information), \mathbf{B}_p encodes the person-specific temporal network, and \mathbf{K}_p encodes the person-specific contemporaneous GGM. Let \mathbf{B}_* and $\mathbf{K}_*^{(\boldsymbol{\Theta})}$ encode the expected temporal and contemporaneous network when selecting a person at random. Furthermore, we can assume without loss of information that data are grand-mean centered. We then obtain

$$\begin{aligned} \mathcal{E}(\boldsymbol{\mu}_P) &= \mathbf{0} \\ \mathcal{E}(\mathbf{B}_P) &= \mathbf{B}_* \\ \mathcal{E}(\mathbf{K}_P^{(\boldsymbol{\Theta})}) &= \mathbf{K}_*. \end{aligned}$$

Here, \mathbf{B}_* and $\mathbf{K}_*^{(\boldsymbol{\Theta})}$ now encode the average parameters in the population: the *fixed effects*. Deviations from these fixed effects, such as $\mathbf{B}_p - \mathbf{B}_*$, are often called *random effects*. Besides the individual network structures, researchers often aim to estimate the structure and parameters of these fixed effects because these tell us something about the average intraindividual effect. Researchers also aim to estimate the variance-covariance structure of the random effects because it tell us something about individual differences (Bringmann et al., 2013).

As explained in more detail in Section 3 of the supplementary materials, the random effects can be modeled by assuming a second level normal distribution on all the parameters. This can be complicated, however, especially when modeling partial correlation coefficients in such a way (e.g., any hierarchical model for $\mathbf{K}^{(\Theta)}$ needs to take into account that this matrix must remain positive definite). The interpretation of, for example, correlations between different temporal or contemporaneous edges is also difficult. Therefore, we only focus here on a subset of the parameters where we can easily interpret the second-level model: the mean structure. As a result, if a multivariate normal is assumed for all parameters, then it is also assumed for the marginal distribution of the means—regardless of other parameters:

$$\boldsymbol{\mu} \sim N(\mathbf{0}, \boldsymbol{\Omega}).$$

Again, we can invert the variance–covariance matrix to obtain a GGM,

$$\mathbf{K}^{(\Omega)} = \boldsymbol{\Omega}^{-1},$$

which corresponds to the between-subjects network described above. As such, estimating the graphical VAR model on $n > 1$ time-series analysis allows for the separation of variance into three distinct network structures: temporal networks, contemporaneous networks, and the between-subjects network.

Estimation

Table 3 describes several estimation procedures for the graphical VAR model in $n > 1$ datasets. First, we can estimate a graphical VAR model for every subject to obtain subject-specific estimates for the temporal and contemporaneous networks. Similarly, we can estimate fixed-effects networks by estimating a graphical VAR model on the entire within-subjects centered dataset, using the sample means of every subject on every variable as a plug-in for the within-person means. Consequently, we can estimate the between-subjects network by estimating a GGM on the sample means of each subject on all variables. We can readily apply the LASSO regularization methods described above for this purpose. It is also possible to use the methodology outlined by Abegaz and Wit (2013) to obtain temporal and contemporaneous networks and the glasso algorithm (Friedman et al., 2008) to obtain the between-subjects network. Tuning parameter selection can be achieved by minimizing the EBIC (Abegaz and Wit, 2013; Chen and Chen, 2008; Foygel and Drton, 2010). We term this framework *pooled and individual LASSO estimation* and have implemented an automated function to obtain fixed-effects networks and subject-specific networks in the R package graphicalVAR (Epskamp, 2017b). The performance of pooled and individual LASSO estimation is assessed in simulations reported in section 1.3 of the supplementary materials.

An alternative estimation procedure is to use multilevel modeling (Hamaker, 2012). The benefit of this approach is that instead of estimating the VAR model in each subject, only the fixed effects and variance–covariance of the random effects need to be estimated. This can be done by integrating over the distribution of the random effects or by specifying the model using hierarchical Bayesian Monte-Carlo sampling methods (Gelman and Hill, 2006; Schuurman et al., 2016b). Bayesian estimation has proved to be powerful in estimating such models. However, Bayesian and multivariate maximum likelihood estimation scale up

poorly due to a large number of random-effect correlations and other parameters that need to be estimated. Bringmann et al. (2013) proposed a frequentist estimation procedure that scales up better. In this work, the multilevel VAR model is estimated by sequentially estimating univariate multilevel regression models of one variable given all lagged variables. Doing so ignores several correlations of random effects because many parameters are not estimated in the same model, which simplifies the analysis. For example, only correlations between incoming edges to the same node are included in the univariate models. This method scales up well to approximately six to eight variables when estimating correlated random effects or around 20 variables when estimating orthogonal random effects (or by using a moving window approach; Bringmann et al. 2015).

The methodology of Bringmann et al. (2013) does not estimate contemporaneous or between-subjects networks. To this end, we extended the algorithm in a framework we term *two step multilevel VAR*. The details of this estimation procedure are explained in Section 3 of the supplementary materials. In short, we extend the methodology of Bringmann et al. (2013) by within-person centering and by adding subject sample means as between-subjects predictors (as discussed by e.g., Hoffman and Stawski 2009; Curran and Bauer 2011; Hamaker and Grasman 2014). This allows us to estimate between-subjects networks by collecting regression coefficients as in Equation (5) and to symmetrize the resulting matrix.⁸ In a second step, we take the residuals of the first analysis and again perform sequential univariate multilevel regression models to predict each residual from all other residuals in the same measurement occasion. Again, these can be collected, as in Equation (5), and symmetrized to obtain contemporaneous networks. Fixed-effects networks can be thresholded by removing all effects that are not significant. For the between subjects and contemporaneous networks, this results in two p values for every edge—either both can be required to be significant (“and” rule) or only one (“or” rule). Using the “and” rule means erring more on the side of caution (sparser network), whereas using the “or” rule means erring more on the side of discovery.

The choice of which estimator to use is not trivial and depends on the interests of the researcher. In Table 3 we list some pros and cons of each of the methodologies. In particular, multilevel estimation can be very complicated and does not scale up well. Assuming normally distributed parameters can also be problematic because doing so imposes that subjects can not differ on the structure of the networks, merely on their parameterization. When a parameter (e.g., a temporal edge) is zero in some subjects but nonzero in others, then this parameter can not be normally distributed (the distribution would peak at 0). It is currently hard to properly threshold individual networks obtained in multilevel estimation. Nonetheless, multilevel estimation particularly shines in that when estimating an individual network, researchers can borrow information from other subjects. We have performed simulation studies to assess the performance of two step multilevel VAR compared to pooled and individual LASSO estimation. We report the results of these studies in Section 1.3 of the supplementary materials and the results show that both methods adequately detect the true network structures by increasing sample size. Having more time points per subject helps to estimate the contemporaneous and temporal networks, and having more subjects helps to estimate the between-person networks. Two step multilevel VAR performs well in

⁸Standardizing regression parameters from nodewise multilevel models to partial correlation coefficients does not lead to perfectly identical estimates.

Table 3

Three Methods of Estimating Graphical VAR Models With $n > 1$ Subjects

	Bayesian multilevel	Two-step frequentist multilevel	Pooled and individual LASSO estimation
Software	<i>MPlus</i> 8 (Muthén and Muthén, 2007)	<i>mlVAR</i> (Epskamp et al., 2016b)	<i>graphicalVAR</i> (Epskamp, 2017b); <i>sparseTSCGM</i> (Abegaz and Wit, 2015)
Estimation	Specification of a multivariate hierarchical model (e.g., Schuurman et al. 2016b) in Bayesian estimation software.	(1) Sequential univariate multilevel regression models on previous measurement (similar to Bringmann et al. 2013), with within-person centered lagged variables as predictors and means of all other variables as subject-level predictor. (2) Sequential multilevel regression models using the residuals of (1): residuals of one variable are predicted by residuals of all other variables in the same measurement occasion.	(1) Joint multivariate LASSO estimation with EBIC model selection (Abegaz and Wit, 2013) of within-subjects centered data to obtain fixed effects temporal and contemporaneous networks. (2) glasso algorithm with EBIC model selection (Foygel and Drton, 2010) on sample means of subjects to obtain between-person network. (3) Step (1) repeated for each individual dataset to obtain subject-specific networks
Pros	Borrowing information in individual network estimation from other subjects; all model parameters and random-effect variances and correlations can be estimated; credibility intervals can be obtained; advanced extensions possible.	Borrowing information in individual network estimation from other subjects; scales up well to 8 nodes (correlated random effects) or 20 nodes (orthogonal random effects); many random effect variances correlations can be estimated; fast estimation of individual networks.	Fast estimation of fixed effects; scales up well to large numbers of nodes; model selection in individual networks; temporal and contemporaneous networks obtained in the same analysis.
Cons	Does not scale up well to more than a few nodes; slow estimation; no model selection (thresholding possible via credibility intervals); complicated to estimate contemporaneous random effects.	Slow estimation in larger datasets; no model selection (fixed effects can be thresholded using significance); combination of many different models; does not scale up well past 20 nodes.	Subject specific networks estimated without borrowing information from other subjects; between-subjects network estimated in a different model; very slow to estimate subject-specific networks.

Note. The software listed only concerns user-friendly automated software because all these models could readily be implemented in most programming languages or Bayesian sampler packages.

estimating intraindividual networks when the number of observations are low, but it does not estimate intraindividual structures (which edges are zero).

Finally, when analyzing $n > 1$ data, another option is to estimate structural VAR models instead. A promising estimation procedure to estimate such models over many individuals, while dealing with potential heterogeneity, is “group iterative multiple model estimation” (GIMME; Gates and Molenaar 2012), which is implemented in R using the *gimme* package (Lane et al., 2016). In GIMME, no multilevel structure is imposed and subject-specific networks are allowed to differ in structure. Information from other subjects is borrowed, however, in that the structure of individual networks can be based on other subjects (e.g., an edge can be included because it is present in many other subjects). No shrinkage is induced on the parameter estimates that are nonzero (as would be the case in multilevel or hierarchical Bayesian modeling). A variant of GIMME that estimates the graphical VAR or a combination of structural and graphical VAR models has not yet been developed and could pose a promising estimation technique for future research.

Empirical Example 3: Reanalysis of Möttus et al. (2016)

We reanalyzed the data of Möttus et al. (2016) to provide an empirical example of the multilevel VAR methods described above. This data consists of two independent ESM samples, in which items tapping three of the five Five-Factor Model (neuroticism, extraversion, and conscientiousness; McCrae and John 1992) domains were administered as was an additional question that asked participants how much they had exercised since the preceding measurement occasion. Sample 1 consisted of 26 people providing 1,323 observations in total, and Sample 2 consisted of 62 people providing a total of 2,193 observations. Participants in Sample 1 answered questions three times per day, whereas participants in Sample 2 answered questions five times per day. In both samples, the minimum time between measurements was 2 hrs. For more information about the samples and the specific questions asked, we refer readers to Möttus et al. (2016).

To obtain an easier and more interpretable example, we first only analyzed questions aimed to measure the extraversion trait and the question measuring exercise. This led to five variables of interest: questions pertaining to feeling outgoing, energetic, adventurous, or happy and the question measuring participants’ exercise habits. We analyzed the data using the *mlVAR* package. Because the number of variables was small, we estimated the model using correlated temporal and contemporaneous random effects. We ran the model separately for both samples and computed the fixed effects for the temporal, contemporaneous, and between-subjects networks. Correlations of the edge weights indicated that all three networks showed high correspondence between the two samples (temporal network: 0.82, contemporaneous network: 0.94, between-subjects network: 0.70). Owing to the degree of replicability, we combined the two samples and estimated the model on the combined data.

Figure 6 shows the estimated fixed effects of the temporal, contemporaneous, and between-subjects network. In these figures, only significant edges ($\alpha = 0.05$) are shown. In the contemporaneous and between-subjects networks, an edge was retained if one of the two regressions on which the partial correlation is based was significant (the so-called “or” rule; van Borkulo et al. 2014). These results are in line with the hypothetical example shown in Figure 4: People who exercised were more energetic while exercising and less energetic after exercising. In the between-subjects network, no relationship between exercising and energy

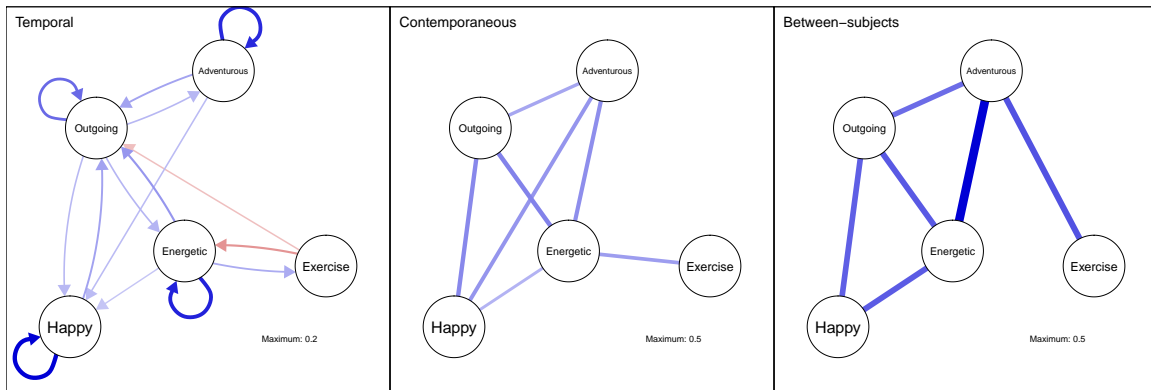


Figure 6. The estimated fixed effects of the three network structures obtainable in multilevel VAR. The model is based on ESM data of 88 people providing a total of 3,516 observations. Due to differences in the scale of the networks, the temporal network was drawn with a different maximum value (i.e., the value indicating the strongest edge in the network) than the contemporaneous and between-subjects networks. Edges that were not significantly different from zero were removed from the networks.

was found. The between-subjects network, however, showed a strong relationship between feeling adventurous and exercising: People who, on average, exercised more also felt, on average, more adventurous. This relationship was not present in the temporal network and much weaker in the contemporaneous network. Also noteworthy is that people were less outgoing after exercising. Figure 7 shows the standard deviation of the random effects in the temporal and contemporaneous networks. Although not many differences can be detected in the temporal network, the contemporaneous network shows strong differences: People mostly differed in their relationship between exercising and feeling energetic.

In addition to using only the extraversion and exercise items, we also ran the model on all 17 administered items in the dataset. In this instance, we used orthogonal random effects to estimate the model because correlated random effects can not be estimated with this large number of variables. Figure 8 shows the estimated fixed effects of the three

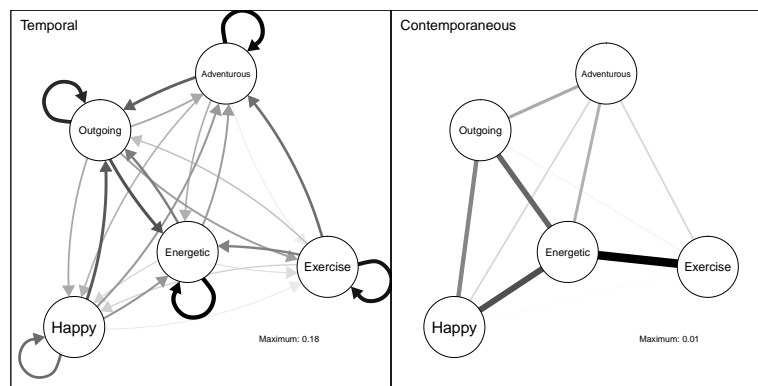


Figure 7. The networks showing the standard deviation of random effects in the temporal and contemporaneous networks. Due to scale differences, networks were plotted using different maximum values.

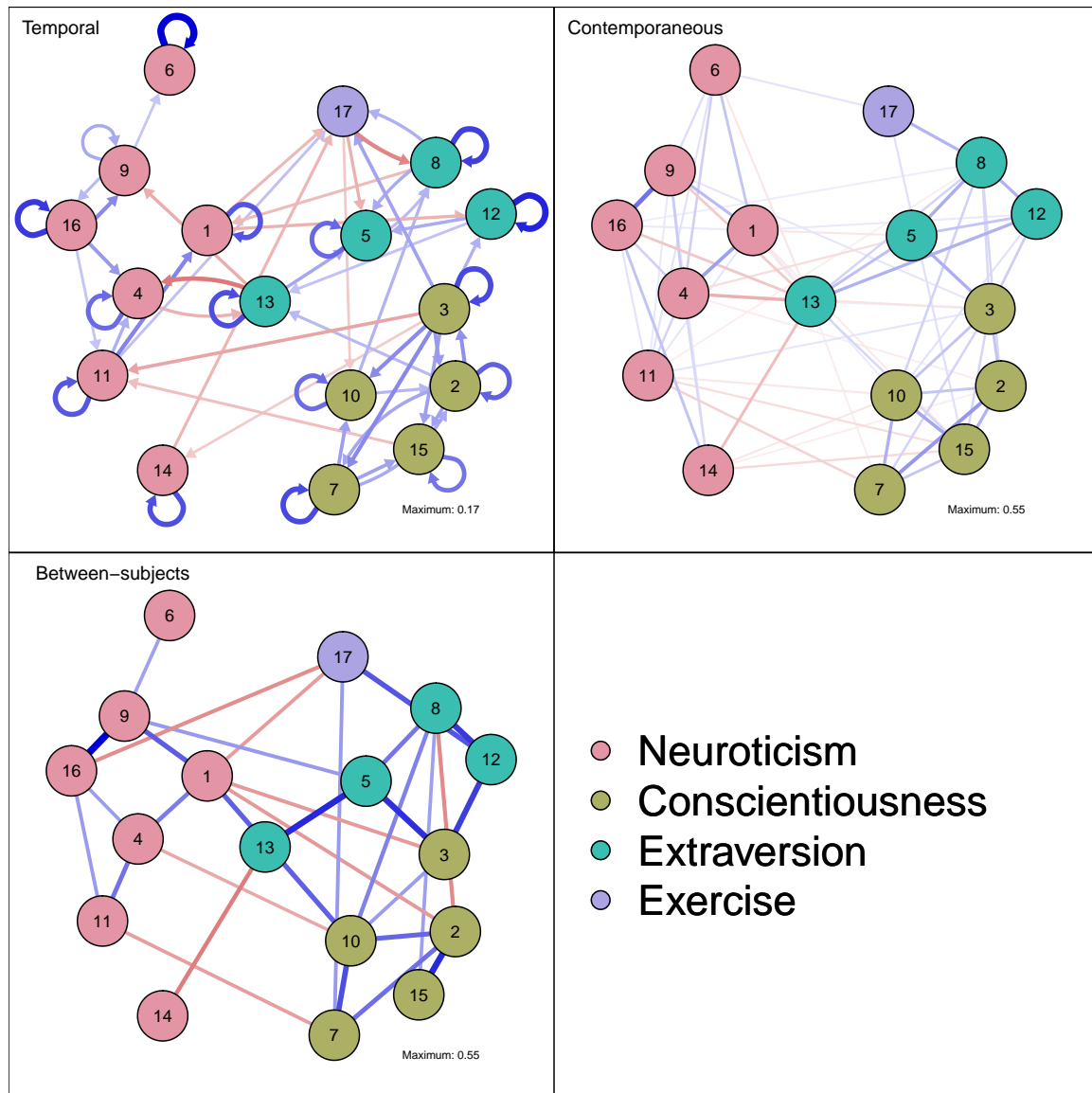


Figure 8. The estimated fixed effects of the three network structures based on all 17 variables administered. Only significant edges are shown. Legend: 1 = “Worried”; 2 = “Organized”; 3 = “Ambitious”; 4 = “Depressed”; 5 = “Outgoing”; 6 = “Self-Conscious”; 7 = “Self-Disciplined”; 8 = “Energetic”; 9 = “Frustrated”; 10 = “Focused”; 11 = “Guilty”; 12 = “Adventurous”; 13 = “Happy”; 14 = “Control”; 15 = “Achieved”; 16 = “Angry”; 17 = “Exercise.”

network structures; it can be seen that indicators of the three traits tend to cluster together in all three networks. Regarding the node exercise, we found the same relationships between exercise, energetic, and adventurous (also found in the previous example) in the larger networks. Furthermore, we noted that exercising was connected to feeling angry in the between-subjects network but not in the other networks. Finally, there was a between-subjects connection between exercising and feeling self-disciplined: People who, on average, exercised more also felt, on average, more self-disciplined.

Empirical Example 4: Reanalysis of Bringmann et al. (2013)

To showcase additional information that can be obtained using the GGM model, we reanalyzed the dataset used and made publicly available by Bringmann et al. (2013), which has been collected by Geschwind et al. (2011). This dataset contains ESM measures of 129 participants, which was collected in two periods over 6 days each: a baseline period and a posttreatment period (mindfulness treatment and a control group). Participants answered 60 measurements per period. Similar to Figure 1 of Bringmann et al. (2013), we analyzed only the baseline dataset on the six items selected by Bringmann et al. (2013). We estimated the networks using both mlVAR (using an “and” rule) and graphicalVAR (using $\gamma = 0.25$). We did not regress the first measurement of the day on the last measurement of the previous day, and removed all pairs of lagged and current variables that contained missing responses. The final sample size was 5,927 observations.

Figure 9 shows the resulting network structures. Unsurprisingly, the temporal networks are very similar to those reported by Bringmann et al. (2013).⁹ Both the temporal and contemporaneous network are in line with what would be expected under a unidimensional auto-correlated latent variable model (many edges selected, low-rank structure, edges of expected sign) with the exception of the positive temporal edge from “fearful” to “pleasant” in the mlVAR networks (which was not selected by graphicalVAR). The between-subjects network was sparser—likely due to it being based on a lower sample size (number of subjects rather than the number of time points). Remarkable is the positive edge between “sad” and “relaxed,” which is based on two significant positive Level 2 regression coefficients ($\beta = 0.202, p = 0.046$ and $\beta = 0.151, p = 0.036$) where the estimated between-subjects correlation is strongly negative (-0.53). This is noteworthy because under a unidimensional factor model, we would not expect partial correlation coefficients to switch sign from marginal correlation coefficients (Holland and Rosenbaum, 1986; van Bork et al., 2016). A possible way the partial correlation coefficient switches sign is if it has been conditioned on one or more common effects between the two variables of interest (in this case, potentially “worry,” “pleasant,” or “fearful”). Of course, these effects must be interpreted with great care, especially given the high p values; we did not control for multiple comparisons, and the same edge is estimated to be weakly negative by graphicalVAR. Still, it is noteworthy that if this edge is weak or nonexistent, the between-subjects structure is still not in line with a unidimensional factor model. In such a factor model, “sad” and “relaxed” (which feature the most connections) would be expected to have a strong negative edge between them (“sad” would have a strong negative factor loading and “relaxed” a strong positive

⁹The networks differ because the estimation of temporal effects differs in that measures are within-subjects centered and subject means are included as Level 2 predictors.

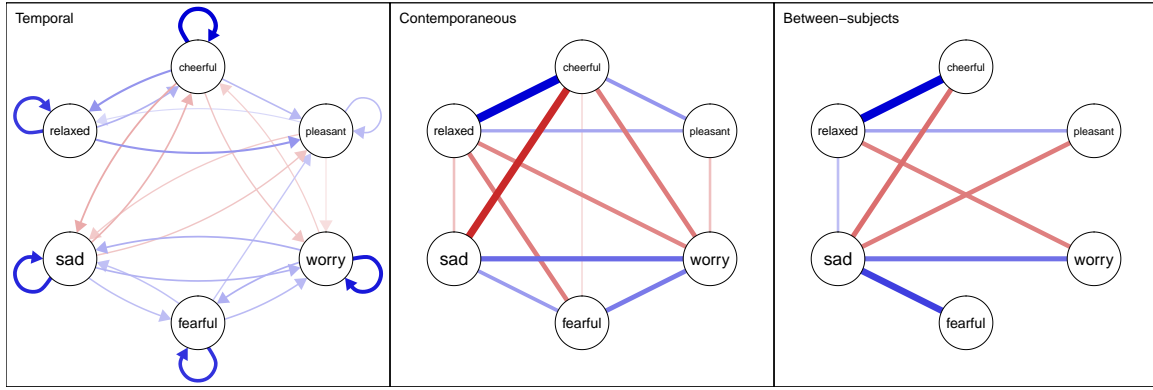
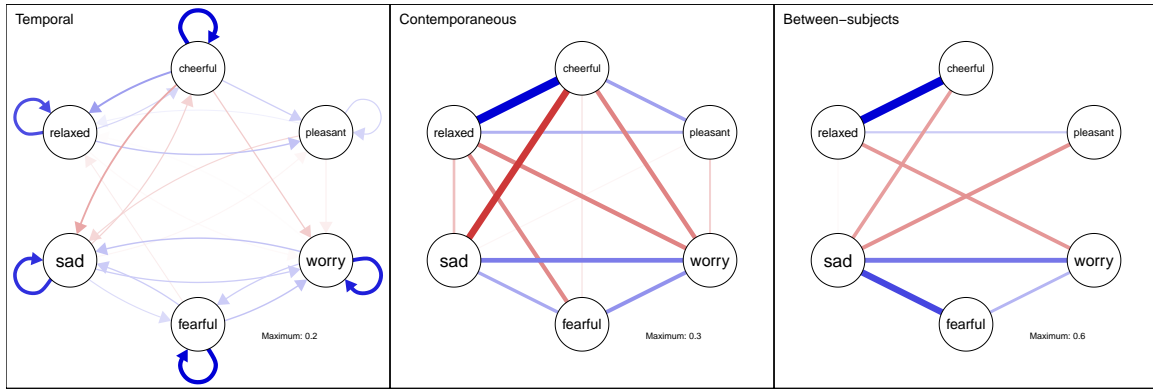
(a) Fixed effect network structures estimated via *mlVAR*(b) Fixed effect network structures estimated via *graphicalVAR*

Figure 9. Reanalysis of the Geschwind et al. (2011) dataset used by Bringmann et al. (2013).

factor loading).

Discussion

We introduced the GGM (Lauritzen 1996), an undirected network model of partial correlation coefficients, and discussed its utility in the analysis of psychological datasets. The GGM presents a promising exploratory data analysis tool because of several reasons: (1) causal effects between variables result in an edge, whereas the lack of a causal effect results in no edge, except in the presence of latent variables or a common effect. The GGM can, therefore, be seen as hypothesis generating because it highlights potential causal pathways. (2) The GGM is well identified, has no equivalent models, and exploratory search algorithms perform well in capturing the true GGM structure. On the other hand, directed network estimation is often poorly identified and leads to edges estimated in the wrong direction. (3) Latent variables emerge in the GGM as low-rank clusters and can also be detected. (4) Edges of the GGM can be interpreted without reliance on a causal hypothesis because the edges show which variables predict each other and because the network structure as a whole shows predictive mediation. (5) But undirected models have been used as data-generating processes and can be interpreted as such.

The GGM can readily be estimated on any dataset that contains multiple observations of the same variables (e.g., multiple people in cross-sectional data or multiple responses in time-series data). LASSO regularization methods perform especially well in estimating such a GGM structure. In temporally ordered data (e.g., $n = 1$ time series), the graphical VAR (Wild et al. 2010) model generalizes the GGM to incorporate temporal effects. We described that two network structures can be obtained: a temporal network, which is a directed network of regression coefficients between lagged and current variables, and a contemporaneous network, which is a GGM describing the relationships that remain after controlling for temporal effects. We argued that both can generate causal hypotheses. In temporally ordered data of multiple subjects (e.g., $n > 1$ time series), the natural combination of cross sectional and time-series data came by adding a third network structure: the between-subjects network, which is a GGM that describes relationships between the stationary means of subjects. We argued that this network can also show potential causal relationships because it might show slower effects than measured in an ESM study and because causal interventions on the means of people (e.g., treatment) are conceivable. We proposed two methods to estimate the three network structures: (1) two step multilevel estimation, which we implemented in the open source R package *mlVAR*, and (2) pooled and individual VAR model estimations using LASSO regularization, which we implemented in the open source R package *graphicalVAR*. We also presented simulation studies showing the performance of these methods.

Limitations and Challenges

The presented methods are not without problems and have several limitations. In regards to multilevel estimation, first, multivariate estimation of the multilevel VAR model is not yet feasible for larger datasets. As such, we only focused on combining univariate models. Doing so, however, means that not all parameters are in the same model. It is important to note that univariate models do not readily provide estimates of the contemporaneous networks, which must be estimated in a second step. Second, even when multivariate estimation is possible, it is still challenging to estimate a multilevel model on contemporaneous networks due to the requirement of positive definite matrices. Third, when more than approximately eight variables are measured, estimating the multilevel models with correlated random effects is no longer feasible in open source MLE software. In this case, orthogonal random effects can be used. Although the simulation study showed that the networks are still attainable when using orthogonal random effects (even though random effects were correlated in the true model), using orthogonal estimation enforces parsimony on the model that may not be plausible. Finally, even when orthogonal estimation is used, the analysis runs very slowly in models with more than 20 variables. As such, multilevel VAR analysis of high-dimensional datasets is not yet feasible. To this end, we discussed pooling within-person centered data and estimating fixed-effects models using LASSO regularization (Abegaz and Wit, 2013). This performed en par with multilevel estimation in higher sample sizes and allows researchers to scale up the analysis more. However, individual network estimation using separate VAR models does not borrow information from other subjects and performs poorly in low sample sizes. Promising developments are new LASSO methods in which shrinkage is attained in penalization rather than hierarchical modeling (Hastie et al., 2015). Future research should investigate the utility of such models in esti-

imating individual network structures that might differ in structure but borrow information from other subjects in its estimation.

These limitations on the estimation methods come with more limitations in the statistical models themselves. VAR modeling, especially, is not without problems and faces severe challenges (Hamaker et al., 2015; Hamaker and Wichers, 2017). We made several assumptions that can be problematic. For instance, in characterizing the likelihood of time-series data, we need to assume that the distribution of variables at time $t - 1$ and time t are the same for all t . That raises two distinct assumptions: (1) The difference in time between measurements are roughly equal, and (2) the parameters do not change over time. Equidistance in time is especially important for the interpretation of temporal networks. Promising work is being done in this area where VAR networks can be estimated on nonequidistant datasets (Driver et al., *ress*; Oravecz et al., 2009; Oud and Jansen, 2000). The assumption of stationarity is needed to estimate structures when data are limited but might not be tenable especially in longer time series (Rovine and Walls, 2006). Promising time-varying estimation procedures are being developed (Bringmann et al., 2016; Haslbeck and Waldorp, 2016a), but are not yet extended to the graphical VAR framework. Furthermore, the interpretation of temporal coefficients when drawn as a network is not without discussion, and several different methods for standardization exist (Bulteel et al., 2016; Schuurman et al., 2016a).¹⁰

Another particularly important assumption made in this paper is that of multivariate normality. Indeed, Equation (1) makes this assumption and all other equations follow from this. The assumption of normality is not without problems (Terluin et al., 2016). However, it is not one that is easily solved. This is because there can be many reasons why data are not normally distributed. When data are not normally distributed, then they can not be explained properly using only the means vector and variance-covariance matrix. As a result, the GGM does not properly characterize the joint likelihood function. Three conceivable ways can lead to data not being distributed normally: (1) the data are measured on a different scale (Stevens, 1946), (2) the data are continuous but do not follow a normal density, and (3) there are nonlinear relationships between variables. In the first case, a different graphical model can be used, such as the Ising model for binary data (Epskamp et al., *ress*; van Borkulo et al., 2014) or a mixed graphical model for categorical and Poisson-distributed variables as well as binary and Gaussian variables (Haslbeck and Waldorp, 2016b). Such models have yet to be extended to time-series analysis, especially in separating temporal and contemporaneous effects as the graphical VAR model does. When data are continuous but not normal, multiple reasons can (again) attribute to this. When the underlying process is normal but the measured variables are on a transformed scale, transforming data back to normal should offer a solution (Liu et al., 2009), but when the process itself is nonnormal, such as skewed residuals, the entire modeling framework does not correctly capture the likelihood. Finally, multivariate normality assumes all relationships between variables are linear. When this is not the case, the GGM and VAR model (which fit linear effects) will not properly describe the data. We encourage future researchers to focus on the problem of normality and to develop new methods of overcoming these challenges.

Finally, it should be noted that all network structures only generate hypotheses and

¹⁰We standardized every dataset before analyzing and used the standardization of Wild et al. (2010) in $n = 1$ and pooled temporal networks.

are in no way confirmatory of causal relationships. The analyses showcased in this paper are exploratory but allow researchers to obtain insights into the predictive relationships present in the data—regardless of theory with respect to the data-generating model. Under the assumptions of multivariate normality, stationarity, and the Lag-1 factorization, the networks show how variables predict each other over time (temporal network), within time (contemporaneous network), and on average (between-subjects network). Furthermore, during the thresholding of edges in the multilevel analyses, we did not apply a correction for multiple testing by default. We deliberately chose this because our aim was to present exploratory hypothesis-generating structures, and not correcting for multiple testing yields greater sensitivity.

Conclusion

This paper provides methodological tools that use the GGM to gain insight into the potential dynamics present in psychological data. The described software packages and estimation methods present the current state-of-the-art in a field that is growing rapidly. Combining the GGM with time-series analysis offers a powerful tool to disentangle contemporaneous and temporal effects (at the within-subjects level) from each other and from between-subjects effects. Using the methodology outlined in this paper, researchers can gain exploratory insight into short term within-subjects variation uncontaminated by longer term or between-subjects variation. Researchers can also gain insight into between-subjects effects uncontaminated by short-term variation. One of the main innovations in this paper stems from the substantial interpretation of contemporaneous and between-subjects effects being potentially causal. Both contemporaneous and between-subjects effects are not without debate (e.g., Borsboom et al. 2003; Hamaker 2012; Markus and Borsboom 2013). To this end, much research on discovering psychological dynamics so far has only investigated within-subjects temporal effects. However, such temporal effects are similarly not without problems. Suppose we found a robust association between X and Y together with the temporal precedence of X (e.g., as in Granger causality) in a time-series analysis; we still would not know whether interventions on X would actually lead to changes in Y . Associations in within-subjects models can be subject to third-variable issues, such as Simpson’s paradox, just as easily as between-subjects models. Correlations remain correlations, whether they come from individual differences or from time series, and rather than categorically preferring one type of data over another, it appears more sensible to let our judgment on optimal inferences depend on the substantive context. The GGM provides a powerful addition to the exploratory toolbox in behavioral research. The GGM is a powerful addition to the exploratory toolbox in behavioral research. Regardless of whether the data are from time series, cross-sectional studies containing time-varying variables, or from other sources, the GGM can be estimated in many situations. It is up to the researcher to decide if conclusions drawn from such an analysis are warranted by the research design and the variables that are modeled.

Acknowledgements

We would like to thank Laura Bringmann, Noémi Schuurman, and Ellen Hamaker for helpful tips and invigorating discussion.

References

- Abegaz, F. and Wit, E. (2013). Sparse time series chain graphical models for reconstructing genetic networks. *Biostatistics*, page kxt005. <http://dx.doi.org/10.1037/a0028566>.
- Abegaz, F. and Wit, E. (2015). *SparseTSCGM: Sparse Time Series Chain Graphical Models (R package version 2.2)*.
- Barber, R. F., Drton, M., and Others (2015). High-dimensional Ising model selection with Bayesian information criteria. *Electronic Journal of Statistics*, 9(1):567–607.
- Bates, D., Mächler, M., Bolker, B., and Walker, S. (2015). Fitting linear mixed-effects models using lme4. *Journal of Statistical Software*, 67(1):1–48. <http://dx.doi.org/10.18637/jss.v067.i01>.
- Bolger, N. and Laurenceau, J. (2013). *Intensive longitudinal methods*. Guilford, New York, NY, USA.
- Borsboom, D. and Cramer, A. O. J. (2013). Network analysis: An integrative approach to the structure of psychopathology. *Annual Review of Clinical Psychology*, 9:91–121.
- Borsboom, D., Cramer, A. O. J., Schmittmann, V. D., Epskamp, S., and Waldorp, L. J. (2011). The small world of psychopathology. *PloS one*, 6(11):e27407.
- Borsboom, D., Mellenbergh, G. J., and Van Heerden, J. (2003). The theoretical status of latent variables. *Psychological Review*, 110(2):203–219.
- Brandt, P. T. and Williams, J. T. (2007). *Multiple time series models*. Number 148. Sage.
- Bringmann, L. F., Hamaker, E. L., Vigo, D. E., Aubert, A., Borsboom, D., and Tuerlinckx, F. (2016). Changing dynamics: Time-varying autoregressive models using generalized additive modeling. *Psychological methods*.
- Bringmann, L. F., Lemmens, L. H., Huibers, M. J., Borsboom, D., and Tuerlinckx, F. (2015). Revealing the dynamic network structure of the beck depression inventory-ii. *Psychological Medicine*, 45(04):747–757.
- Bringmann, L. F., Vissers, N., Wichers, M., Geschwind, N., Kuppens, P., Peeters, F., Borsboom, D., and Tuerlinckx, F. (2013). A network approach to psychopathology: New insights into clinical longitudinal data. *PLOS ONE*, 8(4):e60188.
- Bulteel, K., Tuerlinckx, F., Brose, A., and Ceulemans, E. (2016). Using raw var regression coefficients to build networks can be misleading. *Multivariate behavioral research*, 51(2-3):330–344.
- Chatfield, C. (2016). *The analysis of time series: an introduction*. CRC press, Boca Raton, FL, USA.
- Chen, G., Glen, D. R., Saad, Z. S., Hamilton, J. P., Thomason, M. E., Gotlib, I. H., and Cox, R. W. (2011a). Vector autoregression, structural equation modeling, and their synthesis in neuroimaging data analysis. *Computers in biology and medicine*, 41(12):1142–1155.
- Chen, G., Glen, D. R., Saad, Z. S., Paul Hamilton, J., Thomason, M. E., Gotlib, I. H., and Cox, R. W. (2011b). Vector autoregression, structural equation modeling, and their synthesis in neuroimaging data analysis. *Comput Biol Med*, 41(12):1142–1155.
- Chen, J. and Chen, Z. (2008). Extended bayesian information criteria for model selection with large model spaces. *Biometrika*, 95(3):759–771.
- Costantini, G., Epskamp, S., Borsboom, D., Perugini, M., Möttus, R., Waldorp, L. J., and Cramer, A. O. J. (2015). State of the aRt personality research: A tutorial on network analysis of personality data in R. *Journal of Research in Personality*, 54:13–29.

- Cramer, A. O. J., Sluis, S., Noordhof, A., Wichers, M., Geschwind, N., Aggen, S. H., Kendler, K. S., and Borsboom, D. (2012). Dimensions of normal personality as networks in search of equilibrium: You can't like parties if you don't like people. *European Journal of Personality*, 26(4):414–431.
- Cramer, A. O. J., Waldorp, L., van der Maas, H., and Borsboom, D. (2010). Comorbidity: A Network Perspective. *Behavioral and Brain Sciences*, 33(2-3):137–150.
- Cronbach, L. J. and Meehl, P. E. (1955). Construct validity in psychological tests. *Psychological Bulletin*, 52(4):281–302.
- Curran, P. J. and Bauer, D. J. (2011). The disaggregation of within-person and between-person effects in longitudinal models of change. *Annual review of psychology*, 62:583–619.
- Driver, C. C., Oud, J. H. L., and Voelkle, M. C. (in press). Continuous time structural equation modelling with r package ctsem. *Journal of Statistical Software*.
- Eichler, M. (2007). Granger causality and path diagrams for multivariate time series. *Journal of Econometrics*, 137(2):334–353.
- Epskamp, S. (2016). Regularized Gaussian Psychological Networks: Brief Report on the Performance of Extended BIC Model Selection. *arXiv preprint*, page arXiv:1606.05771.
- Epskamp, S. (2017a). Chapter 12: Discussion: The road ahead. In *Network Psychometrics*.
- Epskamp, S. (2017b). *graphicalVAR: Graphical VAR for Experience Sampling Data (R package version 0.1.6)*.
- Epskamp, S., Borsboom, D., and Fried, E. I. (2016a). Estimating psychological networks and their accuracy: A tutorial paper. *arXiv preprint*, page arXiv:1604.08462.
- Epskamp, S., Cramer, A., Waldorp, L., Schmittmann, V. D., and Borsboom, D. (2012). qgraph: Network visualizations of relationships in psychometric data. *Journal of Statistical Software*, 48(1):1–18.
- Epskamp, S., Deserno, M. K., and Bringmann, L. F. (2016b). *mlVAR: Multi-Level Vector Autoregression*. R package version 0.3.3.
- Epskamp, S. and Fried, E. I. (2016). A primer on estimating regularized psychological networks. *arXiv preprint*, page arXiv:1607.01367.
- Epskamp, S., Maris, G., Waldorp, L., and Borsboom, D. (in press). Network psychometrics. In Irwing, P., Hughes, D., and Booth, T., editors, *Handbook of Psychometrics*. Wiley, New York, NY, USA.
- Epskamp, S., Rhemtulla, M., and Borsboom, D. (2016c). Generalized network psychometrics: Combining network and latent variable models. *arXiv preprint*, page arXiv:1112.5635.
- Epskamp, S., van Borkulo, C. D., Isvoranu, Adela M. Servaas, M. N., van der Veen, D. C., Riese, H., and Cramer, A. O. J. (submitted). Personalized network modeling in psychopathology: The importance of contemporaneous and temporal connections.
- Ferrer, E. (2016). Exploratory approaches for studying social interactions, dynamics, and multivariate processes in psychological science. *Multivariate behavioral research*, 51(2-3):240–256.
- Foygel, R. and Drton, M. (2010). Extended Bayesian information criteria for Gaussian graphical models. *Advances in Neural Information Processing Systems*, 23:2020–2028.
- Fried, E. I., Bockting, C., Arjadi, R., Borsboom, D., Amshoff, M., Cramer, O. J., Epskamp, S., Tuerlinckx, F., Carr, D., and Stroebe, M. (2015). From loss to loneliness:

- The relationship between bereavement and depressive symptoms. *Journal of abnormal psychology*, 124(2):256–265.
- Fried, E. I., Epskamp, S., Nesse, R. M., Tuerlinckx, F., and Borsboom, D. (2016). What are ‘good’ depression symptoms? Comparing the centrality of DSM and non-DSM symptoms of depression in a network analysis. *Journal of Affective Disorders*, 189:314–320.
- Friedman, J. H., Hastie, T., and Tibshirani, R. (2008). Sparse inverse covariance estimation with the graphical lasso. *Biostatistics*, 9(3):432–441.
- Friedman, J. H., Hastie, T., and Tibshirani, R. (2014). *glasso: Graphical lasso- estimation of Gaussian graphical models (R package version 1.8)*.
- Gates, K. M. and Molenaar, P. C. (2012). Group search algorithm recovers effective connectivity maps for individuals in homogeneous and heterogeneous samples. *NeuroImage*, 63(1):310–319.
- Gates, K. M., Molenaar, P. C., Hillary, F. G., Ram, N., and Rovine, M. J. (2010). Automatic search for fmri connectivity mapping: an alternative to granger causality testing using formal equivalences among sem path modeling, var, and unified sem. *Neuroimage*, 50(3):1118–1125.
- Gelman, A. and Hill, J. (2006). *Data analysis using regression and multilevel/hierarchical models*. Cambridge University Press, New York, NY, USA.
- Geschwind, N., Peeters, F., Drukker, M., van Os, J., and Wichers, M. (2011). Mindfulness training increases momentary positive emotions and reward experience in adults vulnerable to depression: a randomized controlled trial. *Journal of consulting and clinical psychology*, 79(5):618–628.
- Goldberg, L. (1993). The Structure of Phenotypic Personality Traits. *American Psychologist*, 48(1):26–34.
- Golino, H. F. and Epskamp, S. (2016). Exploratory graph analysis: a new approach for estimating the number of dimensions in psychological research. Retrieved from <https://arxiv.org/abs/1605.02231>.
- Granger, C. W. J. (1969). Investigating causal relations by econometric models and cross-spectral methods. *Econometrica: Journal of the Econometric Society*, pages 424–438.
- Hamaker, E., Ceulemans, E., Grasman, R., and Tuerlinckx, F. (2015). Modeling affect dynamics: State of the art and future challenges. *Emotion Review*, 7(4):316–322.
- Hamaker, E. L. (2012). Why researchers should think “within-person”: A paradigmatic rationale. In Mehl, M. R. and Conner, T. S., editors, *Handbook of research methods for studying daily life*, pages 43–61. Guilford Press, New York, NY.
- Hamaker, E. L. and Grasman, R. P. (2014). To center or not to center? investigating inertia with a multilevel autoregressive model. *Frontiers in Psychology*, 5:1492.
- Hamaker, E. L. and Wichers, M. (2017). No time like the present. *Current Directions in Psychological Science*, 26(1):10–15.
- Hamilton, J. D. (1994). *Time series analysis*, volume 2. Princeton university press, Princeton, NJ, USA.
- Haslbeck, J. M. B. and Waldorp, L. J. (2016a). mgm: Structure estimation for time-varying mixed graphical models in high-dimensional data. *arXiv preprint*, page arXiv:1510.06871.
- Haslbeck, J. M. B. and Waldorp, L. J. (2016b). Structure estimation for mixed graphical models in high dimensional data. *arXiv preprint*, page arXiv:1510.05677.

- Hastie, T., Tibshirani, R., and Wainwright, M. (2015). *Statistical learning with sparsity: the lasso and generalizations*. CRC Press, Boca Raton, FL, USA.
- Hayduk, L. A. (2009). Finite feedback cycling in structural equation models. *Structural Equation Modeling*, 16(4):658–675.
- Hoffman, L. and Stawski, R. S. (2009). Persons as contexts: Evaluating between-person and within-person effects in longitudinal analysis. *Research in Human Development*, 6(2-3):97–120.
- Holland, P. W. and Rosenbaum, P. R. (1986). Conditional association and unidimensionality in monotone latent variable models. *The Annals of Statistics*, pages 1523–1543.
- Ising, E. (1925). Beitrag zur theorie des ferromagnetismus. *Zeitschrift für Physik A Hadrons and Nuclei*, 31(1):253–258.
- Isvoranu, A. M., Borsboom, D., van Os, J., and Guloksuz, S. (2016a). A Network Approach to Environmental Impact in Psychotic Disorders: Brief Theoretical Framework. *Schizophrenia Bulletin*, 42(4):870–873.
- Isvoranu, A. M., van Borkulo, C. D., Boyette, L., Wigman, J. T. W., Vinkers, C. H., Borsboom, D., and GROUP Investigators (2016b). A Network Approach to Psychosis: Pathways between Childhood Trauma and Psychotic Symptoms. *Schizophrenia Bulletin*. Advance Access published May 10, 2016.
- Kalisch, M. and Bühlmann, P. (2007). Estimating high-dimensional directed acyclic graphs with the pc-algorithm. *Journal of Machine Learning Research*, 8(Mar):613–636.
- Kalisch, M., Mächler, M., Colombo, D., Maathuis, M. H., and Bühlmann, P. (2012). Causal inference using graphical models with the r package pcalg. *Journal of Statistical Software*, 47(11):1–26.
- Kaplan, D. (2000). *Structural equation modeling: Foundations and extensions*. Sage, Thousand Oaks, CA, USA.
- Kim, C.-J. and Nelson, C. R. (1999). *State-space models with regime switching: classical and Gibbs-sampling approaches with applications*. The MIT press, Cambridge, MA, USA.
- Koller, D. and Friedman, N. (2009). *Probabilistic graphical models: Principles and techniques*. MIT press, Cambridge, MA, USA.
- Kossakowski, J. J., Epskamp, S., Kieffer, J. M., van Borkulo, C. D., Rhemtulla, M., and Borsboom, D. (2015). The application of a network approach to health-related quality of life (HRQoL): Introducing a new method for assessing hrqol in healthy adults and cancer patient. *Quality of Life Research*, 25:781–92.
- Kossakowski, J. J., Groot, P. C., Haslbeck, J. M. B., Borsboom, D., and Wichers, M. (2017). Data from ‘critical slowing down as a personalized early warning signal for depression’. *Journal of Open Psychology Data*, 5:1.
- Krämer, N., Schäfer, J., and Boulesteix, A.-L. (2009). Regularized estimation of large-scale gene association networks using graphical gaussian models. *BMC Bioinformatics*, 10(1):1–24.
- Lane, S., Gates, K., Molenaar, P., Hallquist, M., and Pike, H. (2016). *gimme: Group Iterative Multiple Model Estimation*. R package version 0.1-7.
- Lauritzen, S. L. (1996). *Graphical models*. Clarendon Press, Oxford, UK.
- Liu, H., Lafferty, J. D., and Wasserman, L. (2009). The nonparanormal: Semiparametric estimation of high dimensional undirected graphs. *The Journal of Machine Learning Research*, 10:2295–2328.

- Lord, F. M., Novick, M. R., and Birnbaum, A. (1968). *Statistical theories of mental test scores*. Addison-Wesley, Oxford, UK.
- MacCallum, R. C., Wegener, D. T., Uchino, B. N., and Fabrigar, L. R. (1993). The problem of equivalent models in applications of covariance structure analysis. *Psychological Bulletin*, 114(1):185–199.
- Marchetti, G. M., Drton, M., and Sadeghi, K. (2015). *ggm: Functions for graphical Markov models (R package version 2.3)*.
- Markus, K. A. and Borsboom, D. (2013). *Frontiers of test validity theory: Measurement, causation, and meaning*. Routledge, New York, NY, USA.
- McCrae, R. R. and Costa, P. T. (1997). Personality trait structure as a human universal. *American Psychologist*, 52(5):509–516.
- McCrae, R. R. and John, O. P. (1992). An introduction to the five-factor model and its applications. *Journal of Personality*, 60(2):175–215.
- McNally, R. J., Robinaugh, D. J., Wu, G. W., Wang, L., Deserno, M. K., and Borsboom, D. (2015). Mental disorders as causal systems a network approach to posttraumatic stress disorder. *Clinical Psychological Science*, 3(6):836–849.
- Meinshausen, N. and Bühlmann, P. (2006). High-dimensional graphs and variable selection with the lasso. *The Annals of Statistics*, 34(3):1436–1462.
- Mohammadi, A. and Wit, E. C. (2015). Bdgraph: An r package for bayesian structure learning in graphical models. *arXiv preprint*, page arXiv:1501.05108.
- Molenaar, P. C. (2004). A manifesto on psychology as idiographic science: Bringing the person back into scientific psychology, this time forever. *Measurement*, 2(4):201–218.
- Möttus, R., Epskamp, S., and Francis, A. (2016). Within-and between individual variability of personality characteristics and physical exercise. *Journal of Research in Personality*.
- Murphy, K. P. (2012). *Machine learning: A probabilistic perspective*. MIT press, Cambridge, MA, USA.
- Muthén, L. K. and Muthén, B. O. (2007). Mplus. *Statistical analysis with latent variables. Version*, 3.
- Myin-Germeys, I., Oorschot, M., Collip, D., Lataster, J., Delespaul, P., and van Os, J. (2009). Experience sampling research in psychopathology: Opening the black box of daily life. *Psychological medicine*, 39(09):1533–1547. <http://dx.doi.org/10.1017/S0033291708004947>.
- Oravecz, Z., Tuerlinckx, F., and Vandekerckhove, J. (2009). A hierarchical ornstein–uhlenbeck model for continuous repeated measurement data. *Psychometrika*, 74(3):395–418.
- Oud, J. H. and Jansen, R. A. (2000). Continuous time state space modeling of panel data by means of sem. *Psychometrika*, 65(2):199–215.
- Pearl, J. (2000). *Causality: Models, Reasoning, and Inference*. Cambridge University Press, New York, NY.
- Pourahmadi, M. (2011). Covariance estimation: The glm and regularization perspectives. *Statistical Science*, 26(3):369–387.
- Quax, R., Kandhai, D., and Sloot, P. M. (2013). Information dissipation as an early-warning signal for the lehman brothers collapse in financial time series. *Scientific reports*, 3(1898).
- R Core Team (2016). *R: A Language and Environment for Statistical Computing*. R Foundation for Statistical Computing, Vienna, Austria.

- Revelle, W. (2010). *psych: Procedures for Psychological, Psychometric, and Personality Research (R package version 1.0-93)*. Northwestern University, Evanston, Illinois.
- Rhemtulla, M., Fried, E. I., Aggen, S. H., Tuerlinckx, F., Kendler, K. S., and Borsboom, D. (2016). Network analysis of substance abuse and dependence symptoms. *Drug and alcohol dependence*, 161:230–237.
- Rigdon, E. E. (1995). A necessary and sufficient identification rule for structural models estimated in practice. *Multivariate Behavioral Research*, 30(3):359–383.
- Rosmalen, J. G., Wenting, A. M., Roest, A. M., de Jonge, P., and Bos, E. H. (2012). Revealing causal heterogeneity using time series analysis of ambulatory assessments: application to the association between depression and physical activity after myocardial infarction. *Psychosomatic medicine*, 74(4):377–386.
- Rothman, A. J., Levina, E., and Zhu, J. (2010). Sparse multivariate regression with covariance estimation. *Journal of Computational and Graphical Statistics*, 19(4):947–962.
- Rovine, M. J. and Walls, T. A. (2006). Multilevel autoregressive modeling of interindividual differences in the stability of a process. *Models for intensive longitudinal data*, pages 124–147.
- Schäfer, J., Opgen-Rhein, R., Zuber, V., Ahdesmäki, M., Silva, A. P. D., and Strimmer, K. (2015). *corpcor: Efficient Estimation of Covariance and (Partial) Correlation (R package version 1.6.8)*.
- Schmiedek, F., Lövdén, M., and Lindenberger, U. (2010). Hundred days of cognitive training enhance broad cognitive abilities in adulthood: Findings from the cogito study. *Frontiers in aging neuroscience*, 2:27.
- Schmittmann, V. D., Cramer, A. O. J., Waldorp, L. J., Epskamp, S., Kievit, R. A., and Borsboom, D. (2013). Deconstructing the construct: A network perspective on psychological phenomena. *New Ideas in Psychology*, 31(1):43–53.
- Schuurman, N. K., Ferrer, E., de Boer-Sonnenschein, M., and Hamaker, E. L. (2016a). How to compare cross-lagged associations in a multilevel autoregressive model. *Psychological methods*, 21(2):206.
- Schuurman, N. K., Grasman, R. P. P. P., and Hamaker, E. L. (2016b). A comparison of inverse-wishart prior specifications for covariance matrices in multilevel autoregressive models. *Multivariate Behavioral Research*, 51(2-3):185–206. <http://dx.doi.org/10.1080/00273171.2015.1065398>.
- Scutari, M. (2010). Learning Bayesian Networks with the bnlearn R Package. *Journal of Statistical Software*, 35(3):1–22.
- Shumway, R. H. and Stoffer, D. S. (2010). *Time series analysis and its applications: with R examples*. Springer Science & Business Media, New York, NY, USA.
- Stevens, S. S. (1946). On the theory of scales of measurement. *Science, New Series*, 103(2684):677–680.
- Terluin, B., de Boer, M. R., and de Vet, H. C. (2016). Differences in connection strength between mental symptoms might be explained by differences in variance: Reanalysis of network data did not confirm staging. *PloS one*, 11(11):e0155205.
- Tibshirani, R. (1996). Regression shrinkage and selection via the lasso. *Journal of the Royal Statistical Society. Series B (Methodological)*, 58:267–288.
- van Bork, R., Grasman, R. P. P. P., and Waldorp, L. J. (2016). Unidimensional factor

- models imply weaker partial correlations than zero-order correlations. Retrieved from <https://arxiv.org/abs/1610.03375>.
- van Borkulo, C. D., Borsboom, D., Epskamp, S., Blanken, T. F., Boschloo, L., Schoevers, R. A., and Waldorp, L. J. (2014). A new method for constructing networks from binary data. *Scientific Reports*, 4(5918):1–10.
- van Borkulo, C. D., Boschloo, L., Borsboom, D., Penninx, B. W. J. H., Waldorp, L. J., and Schoevers, R. A. (2015). Association of symptom network structure with the course of depression. *JAMA Psychiatry*, 72(12):1219–1226.
- van der Maas, H. L., Dolan, C. V., Grasman, R. P., Wicherts, J. M., Huizenga, H. M., and Raijmakers, M. E. (2006). A dynamical model of general intelligence: The positive manifold of intelligence by mutualism. *Psychological Review*, 113(4):842–861.
- Wichers, M., Groot, P. C., Psychosystems, ESM Group, and EWS Group (2016). Critical Slowing Down as a Personalized Early Warning Signal for Depression. *Psychotherapy and psychosomatics*, 85(2):114–116.
- Wigman, J., van Os, J., Borsboom, D., Wardenaar, K., Epskamp, S., Klippel, A., Viechtbauer, W., Myin-Germeys, I., and Wichers, M. (2015). Exploring the underlying structure of mental disorders: Cross-diagnostic differences and similarities from a network perspective using both a top-down and a bottom-up approach. *Psychological Medicine*, 45(11):2375–2387.
- Wild, B., Eichler, M., Friederich, H.-C., Hartmann, M., Zipfel, S., and Herzog, W. (2010). A graphical vector autoregressive modeling approach to the analysis of electronic diary data. *BMC Medical Research Methodology*, 10(1):28.
- Witten, D. M., Friedman, J. H., and Simon, N. (2011). New insights and faster computations for the graphical lasso. *Journal of Computational and Graphical Statistics*, 20(4):892–900.
- Woodward, J. (2005). *Making things happen: A theory of causal explanation*. Oxford University Press, Oxford, UK.
- Wright, S. (1921). Correlation and causation. *Journal of agricultural research*, 20(7):557–585.
- Yuan, M. and Lin, Y. (2007). Model selection and estimation in the gaussian graphical model. *Biometrika*, 94(1):19–35.
- Zhao, T., Li, X., Liu, H., Roeder, K., Lafferty, J., and Wasserman, L. (2015). *huge: High-Dimensional Undirected Graph Estimation (R package version 1.2.7)*.

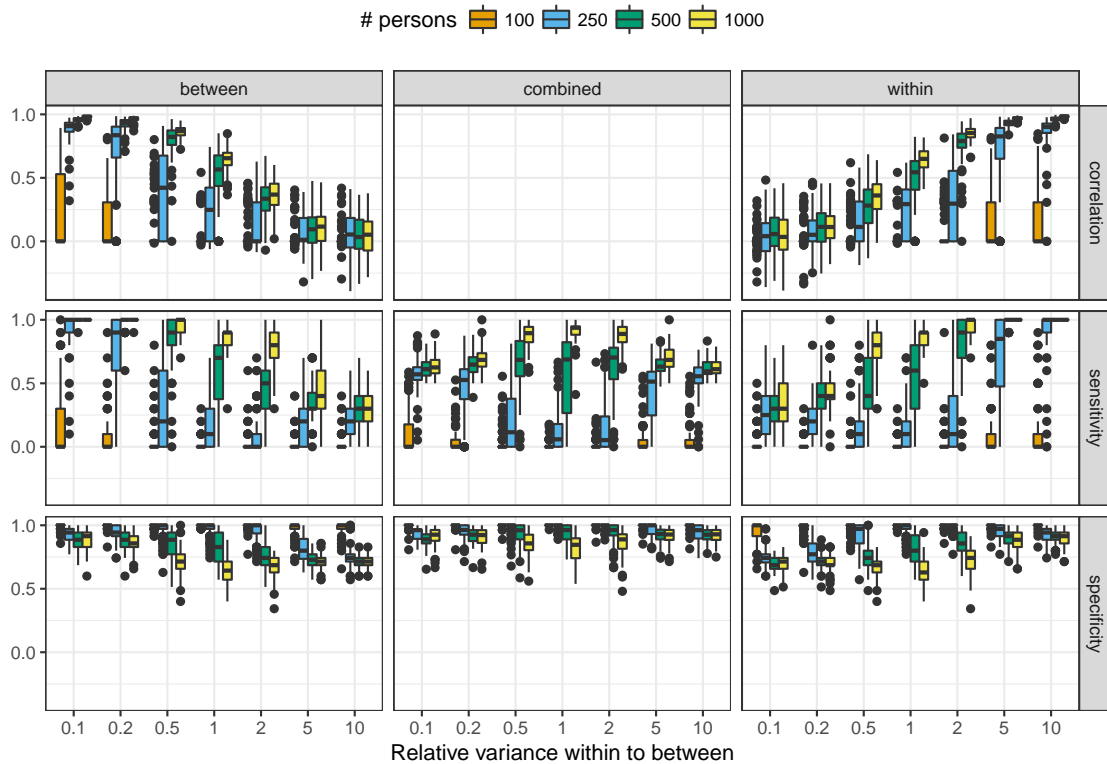


Figure S1. Simulations study showing the performance of cross-sectional analysis. Data were generated by summing scores generated from two distinct distributions: a chain graph GGM (within-person) and a random graph GGM (between-person). Left panels show performance compared to the between-subjects network and right panels show performance compared to the within-subjects network. The center panels show performance compared to an unweighted graph that contained an edge if there was an edge in the within-subjects network or the between-subjects network.

Simulation Studies

Simulation Study 1: Cross-sectional Analysis and Repeated Measures

To investigate the interpretability of cross-sectional data we performed a simulation study. We simulated two network structures: for the within-person network we simulated a chain graph (as shown in Figure S4, panel (b)) in which each edge-weight was set to 0.25 and made negative with 50% probability. For the between-person network, we simulated the same structure but randomly rewired all the edges, such that a random graph was obtained (as shown in Figure S4, panel (c)). Next, the within-person network was scaled such that the within-person variance of all nodes was 0.1, 0.2, 0.5, 1, 2, 5 or 10. The between-subjects variance was set to 1. We estimated the network structure using glasso in combination with EBIC model selection (Foygel and Drton, 2010), as implemented in the *qgraph* package (Epskamp et al., 2012; Epskamp and Fried, 2016). We set the EBIC hyperparameter γ to 0.25.

Figure S1 shows the results, in which the estimated network was compared to the true within and between subjects networks as well as an unweighted network that contained an edge whenever there was an edge in either true network. We did not compute the correlation of edge weights with the unweighted graph as it contained no weights. The figure shows that in large differences between within-person and between-person variance the cross-sectional analysis converges to one of the two networks. When the between-subjects variance was relatively high the within-subjects network was not retrievable and vice versa. When the two variances were approximately equal, edges were detected that were in either of the networks (high sensitivity in the combined graph) and not many edges were detected that were not present in either network (high specificity). This indicates that detected edges in a cross-sectional network can be interpreted to likely represent an edge in the within-subjects network or in the between-subjects network. As such, cross-sectional networks can also be indicative of potential causal pathways—especially when one adheres to possible causal relationships in the between-person network as we argued above—although one should do so with much care. It should be noted that specificity did go down with increased sample size, as the true network does not necessarily contain zeros anymore due to the complex function shown above. These false edges were usually estimated to be very weak. Finally, these results are based on a simulation study in which the within- and between-subject networks completely differed from each other. Preliminary results, such as the empirical samples in this paper, seem to suggest this is not the case in empirical data. We expect cross-sectional data analysis to perform better when the two network structures align.

In order to start disentangling within- and between-subjects variance, one needs an estimate of the person-specific mean. The simplest way to obtain this is by averaging two repeated measures. To this end, we repeated the simulation study above using the exact same setup, but now generated two responses per subject. Next, we within-subject centered the data to compute a within-subject network and used the sample means per subject to compute a between-subjects network. Figure S2 shows that the within-subject network could now be well retrieved, while the between-subject network could only be retrieved when the between-subject variance was large. This seems to suggest that now the estimated network structure can be more reliably interpreted to not be confounded by between-subjects variance. Care should still be taken in interpreting such results, as, for instance, the analysis does assume no individual differences in network structure (which one can not expect to obtain with only two repeated measures).

Simulation Study 2: Graphical VAR and Structural VAR

We performed a simulation study to assess the performance of model selection in structural VAR and graphical VAR. We simulated 1,200 datasets under the structural VAR model shown in Panel (a) of Figure S3. Contemporaneous effects were set to 0.25, residual standard deviations were set to 0.1, temporal autoregressions were varied between 0, 0.1, 0.25 and 0.5 and the number of time points were varied between 100, 250 and 500. By replacing observed variables with latent dummy variables (factor loadings set to 1 with no residual variance), the common form for the structural VAR and graphical VAR models can be seen as a SEM model with a GGM on the residuals of endogenous latent variables. Such a modeling framework has recently been proposed and is termed a latent network model (LNM; Epskamp et al. 2016c). The LNM can be estimated in the R package *lnnet*,

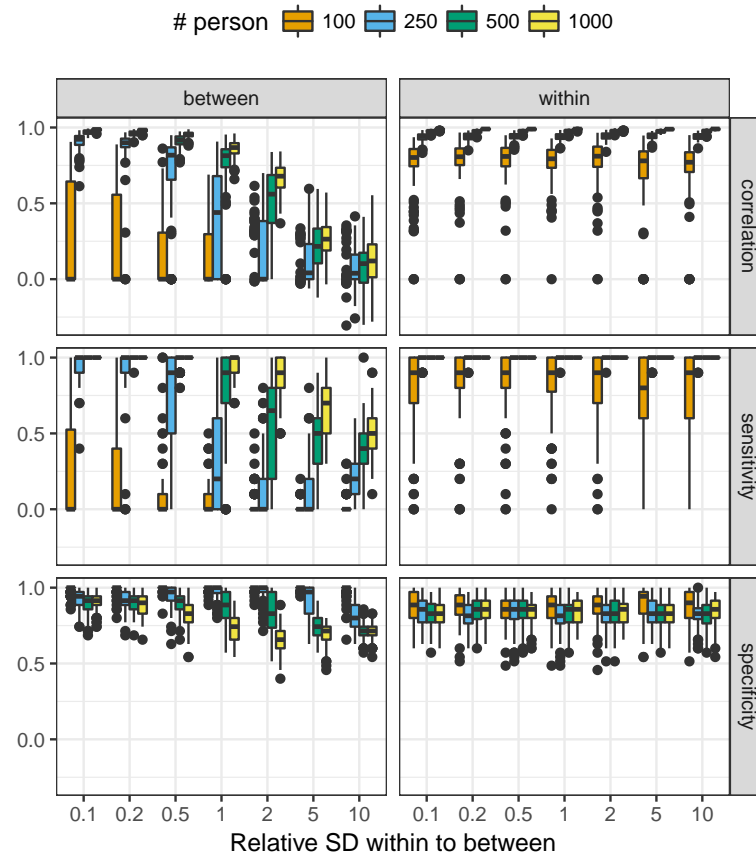


Figure S2. Simulations study showing the performance of cross-sectional analysis. Data were generated by summing scores generated from two distinct distributions: a chain graph GGM (within-person) and a random graph GGM (between-person). Left panels show performance compared to the between-subjects network and right panels show performance compared to the within-subjects network. The center panels show performance compared to an unweighted graph that contained an edge if there was an edge in the within-subjects network or the between-subjects network.

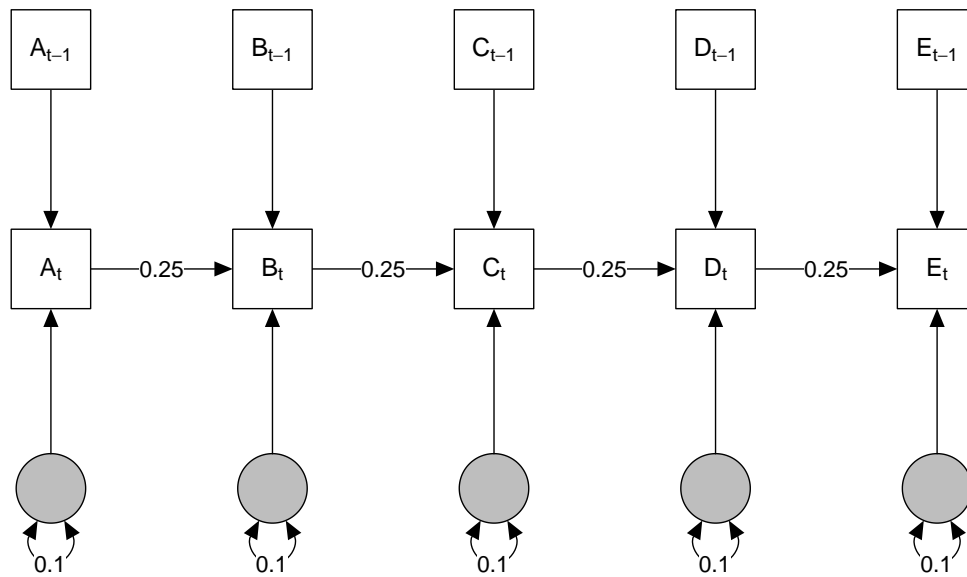
which is at the time of writing the only software package that allows for estimating both the structural VAR and graphical VAR models. We used *lvnet* to perform a stepwise-up model search for both the graphical VAR and structural VAR models on both the temporal and contemporaneous networks (autoregressions were added in the initial model to make the structural VAR models identified). In each step, the edge that improved the BIC the most was added to the model until no edge improved BIC. If two edges improved the BIC equally well, one of the edges were chosen at random. Because in graphical VAR the temporal network has (weak) extra connections, we only investigated the model selection in the contemporaneous network. We computed the *sensitivity* and *specificity* as is common in network estimation studies (e.g., van Borkulo et al. 2014). The sensitivity (also termed *true positive rate*) is high when the method retains edges that are in the true network, and the specificity (also termed *true negative rate*) is high when the method does not retain

edges that are not in the true model (i.e., models without edges that are, in reality, zero).

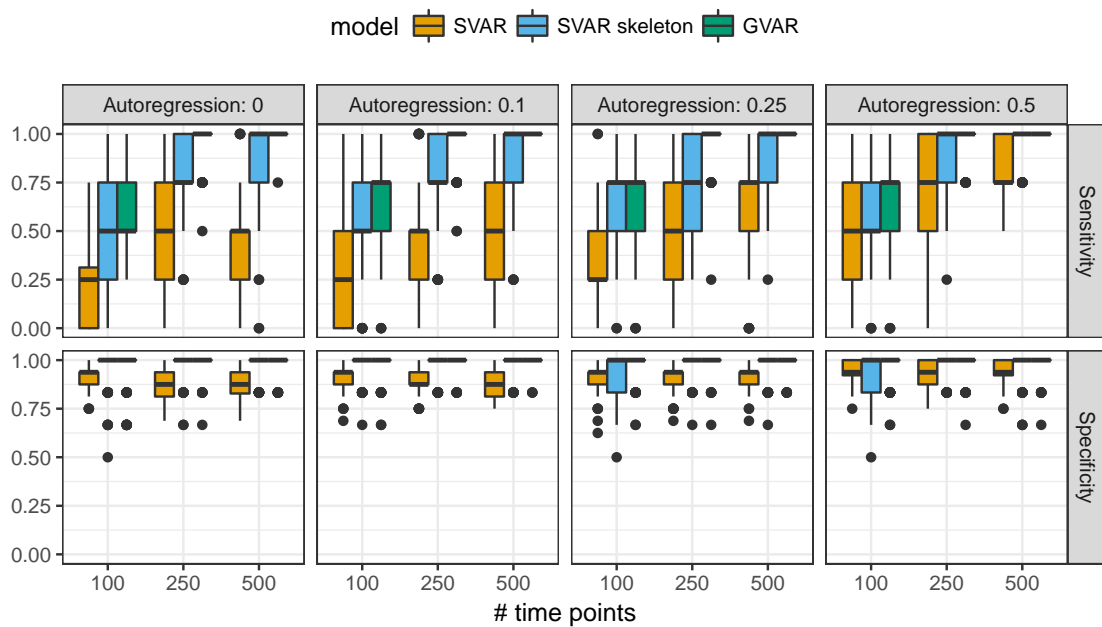
Figure S3 shows the results of this simulation study. Panel (b) shows that graphical VAR outperformed structural VAR in every condition. Structural VAR models feature a lower sensitivity (true edges are not detected) and specificity (edges were detected that were not present in the true model). This was especially true when autoregressions were low, in which case the contemporaneous effects in structural VAR are poorly identified. By analyzing the skeleton of structural VAR models—simply removing direction of the edges—the performance was much better and mostly comparable to graphical VAR models. This indicates that model search in structural VAR often leads to edges being estimated to have the wrong direction (e.g., $A \leftarrow B$ instead of $A \rightarrow B$). Graphical VAR and the structural VAR skeleton do not run this risk. This simulation study was not meant to assess the performance of *lvnet* in estimating these models, because better and faster estimation techniques exist for both modeling frameworks, but to showcase that even though the direction of effect is identified in structural VAR, exploratory estimation might still often lead to a wrong estimation of the direction of causal effect.

Simulation Study 3: Two-step Multi-level VAR and Pooled and Aggregated LASSO Estimation

In this section, we present simulations to assess the performance of *mlVAR* and *graphicalVAR* in performing the above-described methods for estimating network structures on ESM data of multiple subjects. Simulation studies on the described methods for cross-sectional and $n = 1$ studies are available elsewhere (Abegaz and Wit, 2013; Epskamp, 2016; Foygel and Drton, 2010). We simulated ESM data on 8 variables. First, we constructed one temporal, contemporaneous and between-subject network structure as shown in Figure S4, with 50% of non-diagonal parameters made negatively. Then we parameterized the temporal and contemporaneous networks separate per subject. Temporal coefficients and partial contemporaneous or between-subject correlations were drawn from a uniform distribution between 0.2 and 0.5 (or -0.5 and -0.2 for negative edges). The contemporaneous networks and the between-subjects networks were subsequently rescaled such that each node had a residual variance of 0.25 and a between-subjects variance of 1. Thus, temporal and contemporaneous networks were equal in structure (which edge was present and the sign of the edge) but not in weight. To simulate subjects differing in network structure, we rewired intra-individual networks with probability 0 (no differences) or 1 (fully different within-person networks). Sample size and number of observations per subject were varied between 50, 100 and 200, leading to a total of 2 (rewiring) \times 3 (sample size) \times 3 (number of observations per subject) conditions. Each condition was replicated 100 times, leading to 18,00 total simulated datasets. We used both *mlVAR* and *graphicalVAR* to estimate fixed and subject-specific network structures. In *mlVAR*, orthogonal random effects in combination with an “and”-rule were used to threshold significant edges. In *graphicalVAR*, we tested 10×10 tuning parameters (temporal by between) and selected the set of tuning parameters by minimizing the EBIC with $\gamma = 0.25$. To save computing time, we only estimated one individual subject network per replication in the *graphicalVAR* condition (fixed effects were based on all subjects), and thus base the results of individual network estimation performance in both methods on one network per replication. The true fixed effects were set to the mean of all individual networks created.



(a) Structural VAR model under which data were simulated.



(b) Results of the simulation study.

Figure S3. Simulation study to the performance of exploratory search in graphical VAR and structural VAR models. 1,200 simulated datasets under the model shown in Panel (a), with varying temporal autoregressions. Results show the sensitivity (true positive rate) and specificity (true negative rate) of the contemporaneous networks. “SVAR” indicates models estimated by structural VAR, “SVAR skeleton” indicates the same model with the contemporaneous network made undirected and “GVAR” indicates models estimated by graphical VAR.

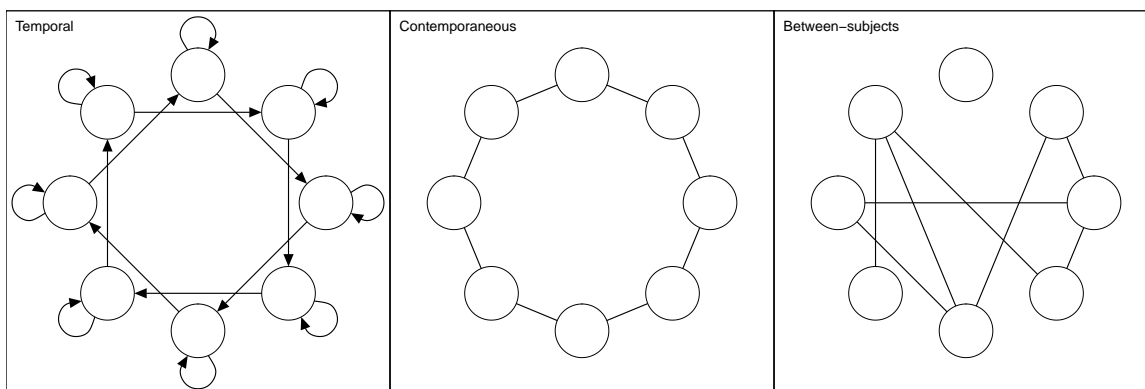


Figure S4. Example of simulated network models in the simulation study. Placing each node in a circle, the temporal network contained positive auto-regressions on each node and one cross-lagged regression on the node two positions to the right, the contemporaneous network was simulated as a chain graph, and the between-subjects network was simulated as a random network with the same number of edges as the contemporaneous network (a different random network was generated for each dataset). Non-diagonal elements were made negative with 50% probability.

In order to assess how well the estimated networks resemble the true networks, we computed for each dataset the correlations between true and estimated fixed temporal, contemporaneous, and between-subjects networks and the correlations between true and estimated subject specific temporal and contemporaneous networks—because the between-subjects network does not have random effects. In line with other studies on assessing how well a method retrieves the structure of a network (e.g., Epskamp et al. 2016c; van Borkulo et al. 2014), we again computed the *sensitivity* (true positive rate) and the *specificity* (true negative rate).

Figure S5 shows the results of the simulation study in the condition where edges were not rewired. It can be seen that performance was generally good in both methods. Fixed effects of the temporal and contemporaneous networks were well estimated (high correlations), most edges in the true network were detected (high sensitivity), and few edges were detected to be nonzero that were, in truth, zero (high specificity). The between-subjects network was better estimated with more people. Using *graphicalVAR* for estimating individual networks showed that at low sample-sizes, the method lacked power to detect true edges (low sensitivity) but did not estimate false edges (high specificity). No model selection is performed in *mlVAR* on subject-specific networks, leading to the specificity of 0 (all edges were always included in the network). The between-subjects estimation using *graphicalVAR* featured a moderate specificity, indicating some false edges were detected. It should be noted that the simulations used EBIC tuning parameter $\gamma = 0.25$, which errs more on the side of discovery than the often used $\gamma = 0.5$ value (Foygel and Drton, 2010). Figure S6 shows the results in the condition where edges were rewired, and shows here too a good performance for both methods. *mlVAR* estimation performed slightly poorer than when the structure was the same over all subjects, and *graphicalVAR* performed identically (as can be expected since no information of other subjects is used in the estimation).

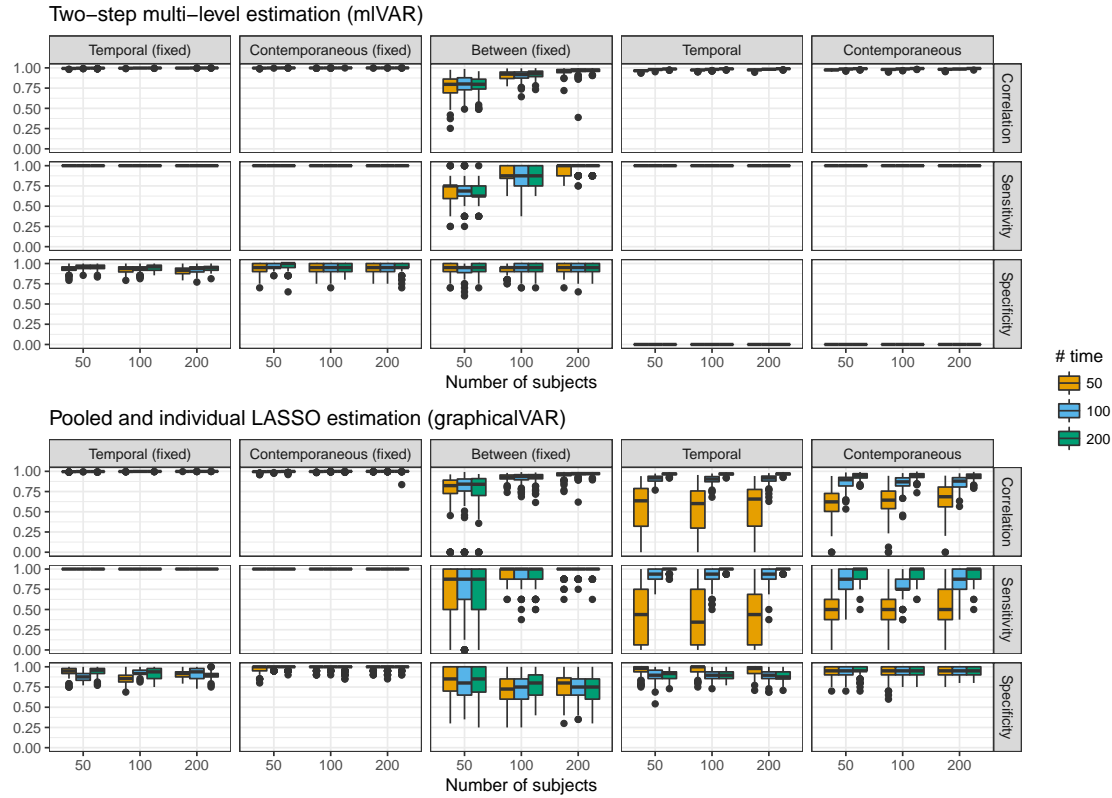


Figure S5. Results of the simulation study using 8 nodes with the same network structure (but different parameters) for each subject. True network structures were generated as shown in Figure S4. Boxplots indicate the distribution of the measures over all the 100 simulated datasets per condition. The left panels relate to the fixed effect structures and the right panels relate to subject specific network structures.

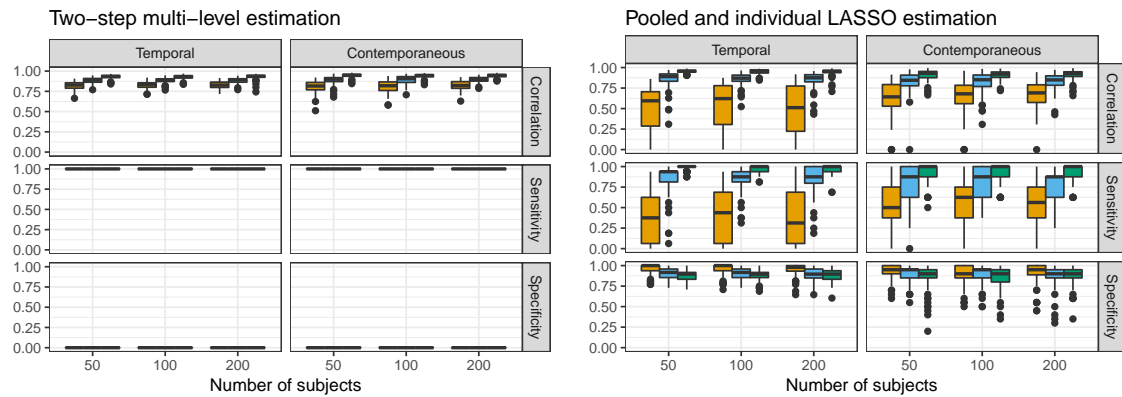


Figure S6. Results of the simulation study using 8 nodes with the differing network structures for each subject. True network structures were generated as shown in Figure S4, but temporal and contemporaneous edges were rewired with 50% probability to other nodes at random. Only subject-specific networks are shown (as the fixed effect structure is ill-defined).

Structural VAR and Graphical VAR

In this appendix we will show the equivalence between structural VAR and graphical VAR. First, we can derive an expression for precision matrix \mathbf{K} :

$$\begin{aligned}\mathbf{K} &= (\mathbf{I} - \mathbf{\Gamma})^\top \mathbf{K}^{(\Theta)} (\mathbf{I} - \mathbf{\Gamma})^\top \\ &= \begin{bmatrix} \mathbf{K}_{11} - \mathbf{\Gamma}_{21}^\top \mathbf{K}_{12} - \mathbf{K}_{12} \mathbf{\Gamma}_{21} + \mathbf{\Gamma}_{21}^\top \mathbf{K}_{22} \mathbf{\Gamma}_{21} & \mathbf{K}_{12}(\mathbf{I} - \mathbf{\Gamma}_{22}) - \mathbf{\Gamma}_{21}^\top \mathbf{K}_{22}(\mathbf{I} - \mathbf{\Gamma}_{22}) \\ (\mathbf{I} - \mathbf{\Gamma}_{22})^\top \mathbf{K}_{21} - (\mathbf{I} - \mathbf{\Gamma}_{22})^\top \mathbf{K}_{22} \mathbf{\Gamma}_{21} & (\mathbf{I} - \mathbf{\Gamma}_{22})^\top \mathbf{K}_{22}(\mathbf{I} - \mathbf{\Gamma}_{22}) \end{bmatrix}\end{aligned}$$

We add superscript (S) to denote a matrix following the structural VAR setup and (G) to denote a matrix following the graphical VAR setup. Then, we obtain:

$$\begin{bmatrix} \mathbf{K}_{11}^{(S)} + \mathbf{\Gamma}_{21}^{(S)\top} \mathbf{K}_{22}^{(S)} \mathbf{\Gamma}_{21}^{(S)} & -\mathbf{\Gamma}_{21}^{(S)\top} \mathbf{K}_{22}^{(S)} (\mathbf{I} - \mathbf{\Gamma}_{22}^{(S)}) \\ -(\mathbf{I} - \mathbf{\Gamma}_{22}^{(S)})^\top \mathbf{K}_{22}^{(S)} \mathbf{\Gamma}_{21}^{(S)} & (\mathbf{I} - \mathbf{\Gamma}_{22}^{(S)})^\top \mathbf{K}_{22}^{(S)} (\mathbf{I} - \mathbf{\Gamma}_{22}^{(S)}) \end{bmatrix} = \begin{bmatrix} \mathbf{K}_{11}^{(G)} + \mathbf{\Gamma}_{21}^{(G)\top} \mathbf{K}_{22}^{(G)} \mathbf{\Gamma}_{21}^{(G)} & -\mathbf{\Gamma}_{21}^{(G)\top} \mathbf{K}_{22}^{(G)} \\ -\mathbf{K}_{22}^{(G)} \mathbf{\Gamma}_{21}^{(G)} & \mathbf{K}_{22}^{(G)} \end{bmatrix}.$$

We can readily find:

$$(\mathbf{I} - \mathbf{\Gamma}_{22}^{(S)})^\top \mathbf{K}_{22}^{(S)} (\mathbf{I} - \mathbf{\Gamma}_{22}^{(S)}) = \mathbf{K}_{22}^{(G)},$$

in which $\mathbf{K}_{22}^{(S)}$ is diagonal. We can recognize this form from equating a causal model to a GGM in the main article. Thus, the contemporaneous GGM in graphicalVAR is the GGM form of the contemporaneous directed network used in structural VAR: it has an undirected edge whenever there is a directed edge or a common effect in the structural VAR model. Next, we can solve for $\mathbf{\Gamma}_{21}^{(G)\top}$:

$$\begin{aligned}-(\mathbf{I} - \mathbf{\Gamma}_{22}^{(S)})^\top \mathbf{K}_{22}^{(S)} \mathbf{\Gamma}_{21}^{(S)} &= -\mathbf{K}_{22}^{(G)} \mathbf{\Gamma}_{21}^{(G)} \\ (\mathbf{I} - \mathbf{\Gamma}_{22}^{(S)})^\top \mathbf{K}_{22}^{(S)} \mathbf{\Gamma}_{21}^{(S)} &= (\mathbf{I} - \mathbf{\Gamma}_{22}^{(S)})^\top \mathbf{K}_{22}^{(S)} (\mathbf{I} - \mathbf{\Gamma}_{22}^{(S)}) \mathbf{\Gamma}_{21}^{(G)} \\ \mathbf{\Gamma}_{21}^{(S)} &= (\mathbf{I} - \mathbf{\Gamma}_{22}^{(S)}) \mathbf{\Gamma}_{21}^{(G)} \\ (\mathbf{I} - \mathbf{\Gamma}_{22}^{(S)})^{-1} \mathbf{\Gamma}_{21}^{(S)} &= \mathbf{\Gamma}_{21}^{(G)}.\end{aligned}$$

Two-step multi-level VAR

In this appendix, we will outline two-step multi-level VAR, which we propose as a methodology to estimate the graphical VAR model using multi-level estimation. This method builds on the work of (Bringmann et al., 2013), and extends their proposed algorithm by including between-subject effects (Hamaker and Grasman, 2014) and estimating the contemporaneous network by performing a second multi-level estimation on the residuals of the temporal model (the second “step”).

When multiple subjects are measured, we need to characterize the likelihood for every subject. Using the assumptions described above, we can model the time series of a subject p with a subject-specific VAR model:

$$\mathbf{y}_{[T,p]} \mid \mathbf{y}_{[T-1,p]} = \mathbf{y}_{[t-1,p]} \sim N(\boldsymbol{\mu}_p + \mathbf{B}_p (\mathbf{y}_{[t-1,p]} - \boldsymbol{\mu}_p), \boldsymbol{\Theta}_p).$$

Often, however, researchers are not interested in the dynamics of a single participant but rather in the generalizability of dynamics over multiple subjects. To this end, researchers

may want to estimate the average effects and interindividual differences of such intraindividual dynamics. We can model these by using the language of multilevel modeling (Bringmann et al., 2013). For each parameter, we denote the average effect as the *fixed effects*, which we encode with an asterisk, and the person-level deviance from this mean as the *random effects*. The parameter vector of random subject P becomes

$$\begin{bmatrix} \boldsymbol{\mu}_P \\ \text{Vec}(\mathbf{B}_P) \\ \text{Vech}(\boldsymbol{\Theta}_P) \end{bmatrix}$$

in which Vec stacks the columns of a matrix, and Vech does the same but only takes the upper-triangular elements including the diagonal. The random effects are centered on zero:

$$\mathcal{E} \left(\begin{bmatrix} \boldsymbol{\mu}_P \\ \text{Vec}(\mathbf{B}_P) \\ \text{Vech}(\boldsymbol{\Theta}_P) \end{bmatrix} \right) = \begin{bmatrix} \mathbf{0} \\ \text{Vec}(\mathbf{B}_*) \\ \text{Vech}(\boldsymbol{\Theta}_*) \end{bmatrix},$$

such that the fixed effects reflect the population means of the parameters. The variance of the random effects can be interpreted as the *individual differences*.

The fixed effects and random effect variances and covariances can be estimated by estimating a VAR model for every subject, pooling the parameter estimates, and computing the mean (fixed effects) and variance–covariance matrix (random effects distribution). This estimation, however, is separate for every subject. To combine all observations in a single model, we can assign distributions over the parameters; in which case, we make use of multilevel modeling. Assigning distributions has two main benefits. First, instead of having a single parameter per subject, we now only need to estimate the parameters of the distribution. For example, when we model observations from 100 subjects, instead of estimating each parameter 100 times, we now only need to estimate its mean and variance. Second, the multilevel structure acts as a prior distribution in Bayesian estimation procedures—in case we wish to obtain person-specific parameter estimates post hoc. In particular, multilevel modeling leads to *shrinkage*; parameter values that are very different from the fixed effects are likely to be estimated closer to the fixed effect in multilevel modeling than when using a separate model for every subject. For example, if we estimate a certain temporal regression in five people and find the values 1.1, 0.9, 0.7, 1.3, and 10, it is likely that the fifth statistic, 10, is an outlier. Ideally, we would estimate this value to be closer to the other values.

Modeling and estimating a random distribution for the contemporaneous variance–covariance matrix is still a topic for future research and not readily implemented in open-source software. This is mainly because these matrices must be positive definite. We cannot simply assign normal distributions to elements of the contemporaneous (partial) variance–covariance matrix because doing so might lead to nonzero probability of matrices that are not positive definite. Therefore, we do not define this distribution here and merely state that there is some population mean, $\boldsymbol{\Theta}_*$. We assume the means and lagged regression parameters to be normally distributed:

$$\begin{bmatrix} \boldsymbol{\mu}_P \\ \text{Vec}(\mathbf{B}_P) \end{bmatrix} \sim N \left(\mathbf{0}, \begin{bmatrix} \boldsymbol{\Omega}^{(\mu)} & \boldsymbol{\Omega}^{(\mu B)} \\ \boldsymbol{\Omega}^{(B\mu)} & \boldsymbol{\Omega}^{(B)} \end{bmatrix} \right).$$

To summarize, the multilevel VAR model makes use of the following parameters for all subjects:

- \mathbf{B}_* : The average within-person temporal relationships between consecutive time points.
- $\mathbf{\Theta}_*$: The average within-person contemporaneous relationships.
- $\mathbf{\Omega}^{(\mu)}$: The between-person relationships between observed variables.
- $\mathbf{\Omega}^{(\mu B)}$ and $\mathbf{\Omega}^{(B)}$: Individual differences between the temporal relationships and other temporal relationships or the means. Of particular interest is $\sqrt{\text{Diag}(\mathbf{\Omega}^{(B)})}$, which shows the individual differences of each temporal relationship (Bringmann et al., 2013).

For any researcher interested in investigating results of particular subjects, the subject-specific structures are also of interest:

- μ_p : The stationary means of subject p .
- \mathbf{B}_p : The within-person temporal relationships of subject p .
- $\mathbf{\Theta}_p$: The within-person contemporaneous relationships of subject p .

Temporal network. Although multivariate multilevel estimation is possible in theory, it is computationally expensive in practice. For example, when we want to explore potential dynamics in medium-sized ESM datasets on around 10 to 20 variables, multivariate multilevel estimation becomes very slow in both MLE and Bayesian estimation. Therefore, we only describe univariate estimation procedures (Bringmann et al., 2013). Because the joint conditional distribution of $\mathbf{y}_{[T,p]} \mid \mathbf{y}_{[T-1,p]} = \mathbf{y}_{[t-1,p]}$ is normal, it follows that the marginal distribution of every variable is univariate normal and can be obtained by dropping all other parameters from the distribution:

$$y_{[T,p,i]} \mid \mathbf{y}_{[T-1,p]} = \mathbf{y}_{[t-1,p]} \sim N\left(\mu_{[p,i]} + \beta_{[p,i]} \left(\mathbf{y}_{[t-1,p]} - \mu_p\right), \theta_{[p,i]}\right),$$

in which $y_{[T,p,i]}$ denotes the i th element of $\mathbf{y}_{[T,p]}$, $\beta_{[p,i]}$ indicates the row vector of the i th row of \mathbf{B}_p , and $\theta_{[p,i]}$ denotes the i th diagonal element of $\mathbf{\Theta}_p$. When drawn as a temporal network, the edges point to node i . Many software packages do not allow the estimation of μ_p as described above. In this case, the sample means of every subject, $\bar{\mathbf{y}}_p$, can be taken as a substitute for μ_p (Hamaker and Grasman, 2014). The model then becomes a univariate multilevel regression model with within-subject centered predictors, estimable by functions such as the `lmer` in `lme4` (Bates et al., 2015). The Level 1 model becomes

$$\begin{aligned} y_{[t,p,i]} &= \mu_{[p,i]} + \beta_{[p,i]} \left(\mathbf{y}_{[t-1,p]} - \bar{\mathbf{y}}_p\right) + \varepsilon_{[t,p,i]} \\ \varepsilon_{[T,p,i]} &\sim N(0, \theta_{[p,i]}), \end{aligned} \tag{9}$$

and the Level 2 model becomes

$$\begin{bmatrix} \mu_{[P,i]} \\ \beta_{[P,i]} \end{bmatrix} \sim N\left(\begin{bmatrix} 0 \\ \beta_{*i} \end{bmatrix}, \begin{bmatrix} \omega_{\mu_i} & \omega^{(\beta_i \mu_i)^\top} \\ \omega^{(\beta_i \mu_i)} & \Omega^{(\beta_i)} \end{bmatrix}\right).$$

Estimation of such univariate models only requires the numeric approximation of an $I + 1$ dimensional integral, which is much easier to compute. Therefore, sequential estimation using univariate models have been used in estimating multilevel VAR models (Bringmann et al., 2013). A downside, however, is that not all parameters are included in the model. In particular, off-diagonal elements of Θ_p and $\Omega^{(\mu)}$ as well as certain elements of $\Omega^{(\mu B)}$ and $\Omega^{(B)}$ are not obtained. A second downside is that estimating correlated random effects does not work well for models with many predictors. In particular, `lmer` becomes very slow with approximately more than eight predictors. As such, networks with more than eight nodes are hard to estimate. To estimate larger networks (e.g., 20 nodes), we can choose to estimate uncorrelated random effects, which we term *orthogonal estimation*. The performance of orthogonal estimation, although the random effects are in reality correlated, is assessed in the simulation study below.

Between-subjects network. To obtain estimates of between-subject effects, the sample means of every subject, $\bar{\mathbf{y}}_p$ in Equation (9), can be included as predictors at the subject level (except for the mean of the dependent variable; Hamaker and Grasman 2014; Hoffman and Stawski 2009; Curran and Bauer 2011). With this extension, the Level 2 model for the person-specific mean of the i th variable now becomes

$$\mu_{[p,i]} = \gamma_i^{(\mu)} \bar{\mathbf{y}}_{[p,-(i)]} + \varepsilon_{[p,i]}^{(\mu)}, \quad (10)$$

in which we use $\gamma_i^{(\mu)}$ to denote the i th row (without the diagonal element i) of a $I \times I$ matrix $\mathbf{B}^{(\mu)}$, and $\bar{\mathbf{y}}_{[p,-(i)]}$ denotes the vector $\bar{\mathbf{y}}_p$ without the i -th element. Because $\bar{y}_{[p,i]}$ is itself an estimate of $\mu_{[p,i]}$, Equation (10) seems to take the form of a multiple regression model. As such, these estimates can be used, to estimate a GGM between the means (Lauritzen, 1996; Meinshausen and Bühlmann, 2006)—the between-subjects network:

$$\mathbf{K}^{(\mu)} \approx \mathbf{D}^{(\mu)} \left(\mathbf{I} - \mathbf{\Gamma}^{(\mu)} \right),$$

with $d_{ii}^{(\mu)} = 1/\text{Var}(\varepsilon_{[p,i]}^{(\mu)})$. Due to the estimation in a multilevel framework, the resulting matrix will not be perfectly symmetric and must be made symmetric by averaging lower and upper triangular elements. Thus, each edge (i.e., partial correlation) in the between-subjects network is estimated by standardizing and averaging two regression parameters: the parameter denoting how well mean A predicts mean B and the regression parameter denoting how well mean B predicts mean A .

Contemporaneous network. An estimate for contemporaneous networks can be obtained in a second step by investigating the residuals of the multilevel model that estimate the temporal and between-subject effects. These residuals can be used to run multilevel models that predict the residuals of one variable from the residuals of other variables at the same time point. Let $\hat{\varepsilon}_{[t,p,i]}$ denote the estimated residual of variable i at time point t of person p , and let $\hat{\varepsilon}_{[t,p,-(i)]}$ denote the vector of residuals of all other variables at this time point. The Level 1 model then becomes

$$\hat{\varepsilon}_{[t,p,i]} = \gamma_{[p,i]}^{(\Theta)} \hat{\varepsilon}_{[t,p,-(i)]} + \varepsilon_{[t,p,i]}^{(\Theta)}, \quad (11)$$

in which $\gamma_{[p,i]}^{(\Theta)}$ represents the i -th row (without the diagonal element i) of a $I \times I$ matrix, $\mathbf{\Gamma}_p^{(\Theta)}$, and $\varepsilon_{[t,p,i]}^{(\Theta)}$ represents a residual. In the Level 2 model, we again assign a multivariate

normal distribution to parameters in $\gamma_i^{(\Theta)}$. It can be seen that Equation (11) also takes the form of a multiple regression model. Thus, this model can again be seen as the node-wise GGM estimation procedure:

$$K_p^{(\Theta)} \approx D_p^{(\Theta)} (I - \Gamma_p^{(\Theta)}),$$

with $d_{[p,i]}^{(\Theta)} = 1/\text{Var}(\varepsilon_{[T,p,i]}^{(\Theta)})$. Again the matrices need to be made symmetric by averaging upper and lower triangle elements. Fixed effects can be obtained by using the fixed effects matrices instead in the expression above. As with the temporal network, orthogonal estimation can be used when the number of variables is large (i.e., larger than approximately eight).

Thresholding. After estimating network structures, researchers may be interested in removing edges that may be spurious and due to sampling error. By setting edge weights to zero, effectively removing edges from a network, a sparse network is obtained that is more easily interpretable. One method of doing so is by removing all edges that are not significantly different from zero. For fixed effects, multilevel software returns standard errors and p values, allowing this thresholding to be done. For the temporal networks, each edge is represented by one parameter and thus by one p value. The contemporaneous and between-subjects networks, however, are a function of two parameters that are standardized and averaged: a regression parameter for the multiple regression model of the first node and a regression parameter for the multiple regression model of the second node. As such, for every edge, two p values are obtained. We can choose to retain edges of which at least one of the two p values is significant, termed the OR-rule, or we can choose to retain edges in which both p values are significant, termed the AND-rule (Barber et al., 2015).

Summary. In sum, the above described two-step estimation method proposes to estimate a multilevel model per variable, using within-person centered lagged variables as within-subject predictors and the sample means as between-subject predictors. These models can be used to obtain estimates for the temporal network and between-subjects network. In a second step, the contemporaneous networks can be estimated by estimating a second multilevel on the residuals of the first multilevel model. The *mlVAR* R package implements these methods (Epskamp et al., 2016b). In this package, temporal coefficients can be estimated as being “unique” per subject (unique VAR models per subject), “correlated” (estimating correlations between temporal effects), “orthogonal” (assuming temporal effects are not correlated), or “fixed” (no multilevel structure on temporal effects). The contemporaneous effects can also be estimated as being “fixed” (all residuals are used to obtain one GGM), “correlated” (second step multilevel model with correlated random effects), “orthogonal” (second step multilevel model with uncorrelated random effects), or “unique” (residuals are used to obtain a GGM per subject). The *mlVAR* package can also be used to plot the estimated networks, in which significance thresholding is used by default with a significance level of $\alpha = 0.05$.

Stationary distribution

The graphical VAR model implies the following expression for the variance-covariance matrix of \mathbf{y}_t :

$$\begin{aligned} \text{Var}(\mathbf{y}_T) &= \text{Var}(\mathbf{B}\mathbf{y}_{T-1} + \varepsilon_T) \\ \Sigma &= \mathbf{B}\Sigma\mathbf{B}^\top + \Theta, \end{aligned}$$

in which we make use of the assumption of stationarity and the assumption that residuals $\boldsymbol{\varepsilon}_T$ are uncorrelated with \boldsymbol{y}_{T-1} . Now, we can make use of the vectorization operator Vec and the Kronecker product \otimes to obtain (Kim and Nelson, 1999):

$$(\boldsymbol{I} - \boldsymbol{B} \otimes \boldsymbol{B})^{-1} \text{Vec}(\boldsymbol{\Theta}) = \text{Vec}(\boldsymbol{\Sigma}) \quad ,$$

which gives an expression for the elements of $\boldsymbol{\Sigma}$ in terms of \boldsymbol{B} and $\boldsymbol{\Theta}$.